STABILITY AND BIFURCATION ANALYSIS OF A NUTRIENT-PHYTOPLANKTON MODEL

ZAKARIA MOHAMAD

STABILITY AND BIFURCATION ANALYSIS OF A NUTRIENT-PHYTOPLANKTON MODEL

by

©Zakaria Mohamad

A thesis submitted to the

School of Graduate Studies

in partial fulfillment of the

requirements for degree of

Master of Science

Department of Mathematics and Statistics

Memorial University of Newfoundland

September 2008

St. John's Newfoundland Canada

Abstract

This Master thesis consists of six chapters, which are mainly concerned with the stability and bifurcation analysis of a Nutrient (N), Phytoplankton (A) model.

In chapter 1, some existing Nutrient-Phytoplankton models and the motivation for this work are presented.

In chapter 2, we introduce a two dimensional (N, A) model to describe the nutrient-phytoplankton interactions, and investigate the dynamical properties of this model. We show the existence of a boundary equilibrium point, and use geometerical and analytical methods to find conditions for the existence of none, one, or at most two positive equilibrium points. We then analyze the stability of each equilibrium point.

In chapter 3, we modify the previous model by introducing a time delay τ, and discuss its effect on the stability of each equilibrium point, by investigating the distribution of the roots in the corresponding characteristic equation.

In chapter 4, we discuss the bifurcations. By using the projection method, we prove the existence of a saddle-node bifurcation for the system without delay. And by using the center manifold theory and normal form method, we study the direction of Hopf bifurcation and the stability of the periodic solutions for both systems, and we prove the existence of Hopf-Zero bifurcation for the system with delay.

In chapter 5, we provide numerical simulations to verify our theoretical predictions in the previous chapters, and biological interpretations based on these simulations.

In the last chapter, we summarize the results obtained in the previous chapters and provide suggestions to improve the model.

Acknowledgemet

I would like to express my great appreciation to my supervisor Dr. Yuan Yuan for her constant encouragement and advice. She always provided me with valuable comments and useful discussions. She carefully read my work several times, and offered me very valuable suggestions. This work would have been impossible without her guidance and help.

I sincerely acknowledge the financial support provided by my supervisor Dr.Yuan Yuan, the School of Graduate Studies, and the Department of Mathematics and Statistics.

Also, my sincere thank to my professors who have shared with me their wealth of knowledge at various points in the course of my program, especially, Dr. Jie Xiao, Dr. Xiaoqiang Zhao and Dr. Andy Foster for teaching me a variety of graduate courses.

I wish to thank the administrative staff for providing us with the necessary facilities to complete our work. Also, my sincere thank to the graduate students for creating friendly and positive atmosphere.

I also acknowledge the examiners of this thesis, Dr. Gail Wolkowicz and Dr. Chun-Hua Ou for their valuable comments.

Finally, I wish to express my gratitude to my family for their support and encouragement.

Contents

List of Figures

Chapter 1

INTRODUCTION

The theory of dynamical system is used to describe the long term qualitative behavior of a complex real system. The initial state of such a system and the laws governing its evolution are expressed in terms of differential equations. Since many differential equations cannot be solved conveniently by analytical methods, it is important to consider what qualitative information can be obtained about their solutions without actually solving the equations. This approach is geometrical in character and leads to a qualitative understanding of the behavior of solutions rather than detailed quantitative information.

A dynamical system usually has several independent parameters, it is essential to understand the qualitative properties of the system as the parameters vary. Stability and bifurcation analysis are two of the fundamental tasks in dynamical theory. Studying the stability determines whether the system settles down to equilibrium or keeps repeating in cycles. With the varying of system parameters the stability can be lost, then the qualitative properties have significant change which is called a bifurcation.

Bifurcation theory attempts to explain various phenomena that have been discovered and described in the natural sciences over the centuries. The principle theories for dealing with bifurcation analysis at fixed points involve the center manifold and normal form. Both of them are fundamental and rigorous mathematical techniques in the local theory of dynamical systems. They are used to reduce the dimensionality of the system without changing the dynamical behavior.

Dynamics has many applications in a wide range of disciplines, including biology, chemistry, engineering, ecology, economics, and even sociology [1, 2, 3]. The increasing use of mathematics in biology is inevitable as biology becomes more quantitative. Population dynamics is an important subject in mathematical biology, study the long-time behavior of the systems governed by various evolutionary equations represent the interactions of population and its environment. The most widely studied models in population dynamics include predator prey, competition, and cooperation models. In predator prey models, some species serve as food for the others. In competition models several species compete for the same resources, where an increase in the size of either population tends to decrease the growth rate of the other population [4]. In cooperation models different species help each other to exist.

In this thesis we consider the interaction of phytoplankton and nutrient modelled as a predator-prey relationship. Phytoplankton are microscopic plants that live in the surface layer of an ocean, sea, lake, or other body of water. They use inorganic nutrients, such as nitrate and phosphate for growth, and the dead phytoplankton biomass is converted again into nutrients. Phytoplankton form the basis of marine food web and they support the life of all higher marine organisms.

One of the important features associated with a phytoplankton population is the occurrence of phytoplankton bloom, which is a dense populations that occurs in a wide range of water systems, at different times of the year. Biologically, the main reason of phytoplankton bloom is the excessive loading of external nutrients such as nitrogen and phosphorous, which is a result of increasing human population, the extensive development in agricultural, industrial, social and other human activities. Phytoplankton bloom has many biological and commercial hazards. One of its biological impacts is the growth of some toxins, such as the blue green algae, which contaminate water supplies of wild and domestic animals and change the decomposition of various organisms in the environment. One of the commercial hazards of phytoplankton bloom is the unpleasant changes in the odor and the taste of water, which results in loss of human access for swimming, sailing, and other recreational activities.

Studying the interaction of phytoplankton and nutrient is very important in a phytoplankton ecosystem. To better understand and control the phytoplankton bloom, from a mathematical point of view, modeling of the phytoplankton population is an essential tool to improve our understanding of the physical and biological processes that lead to phytoplankton bloom. There are numerous mathematical models describing the dynamics of marine plankton since the pioneering paper of Riley et al [5]. Some paid more attention on the interplay of various physical factors (light, temperature, hydrodynamics), [6, 7, 8]; some focused on the biological factors (nutrient supply, predation), [9, 10, 11, 12]. The chemostat is an experimental system used to simulate the nutrient-phytoplankton interactions in an environment very similar to the natural biological system. It can be used to investigate the role of different factors that affect nutrient-phytoplankton interactions in

a controlled environment. Hsu et al [13], Waltman et al [14], Caperon [15], Powell and Richerson et al [16], Buttler et al [17], Butler and Wolkowicz [18] have proposed models based on chemostat type equations to simulate the growth of phytoplankton communities. However, there is an important difference between a chemostat and a real water system (river, lake or ocean). A real water system has a regeneration of nutrient due to bacterial decomposition of the dead biomass. Nisbet and Gurney [19], Nisbet et al [20], Ulanowicz [21], Powell and Richerson [22] have proposed nutrient-phytoplankton models with instantaneous nutrient recycling. Ruan [23] discussed the effect of both the discrete delay and the distributed delay on dissipativity, stability of the interior equilibrium and persistence. Huppert et al [24] considered a simple nutrient-phytoplankton model to illustrate the dynamical properties of phytoplankton bloom. Apart from simulation studies, they found the effect of a threshold analytically and traced the appearance of bloom depending on the initial condition. Since the simplified model is "far away" from the real system they gave a more general model without any theorical discussion.

All of us know that, in the system of ordinary differential equations (ODE), the future state of the system is independent of the past state and is determined solely by the present. However, it is getting apparent that this gives only the first approximation of the considered real system [25].

From real observation in the natural phytoplankton-nutrient system, it is well known that time is required to regenerate nutrient from dead phytoplankton biomass by bacterial decomposition.

The goal of this thesis is to construct a more realistic nutrient-phytoplankton model, study the dynamical properties including the stability and bifurcation of the model by us-

ing the theory of dynamical system, then provide biological interpretations based on the mathematical results. At first, we construct and analyze a ODE model, then modify the model with delayed nutrient recycling and discuss the effect of time delay. Accordingly, the thesis is organized as follows:

In the next chapter we present the nutrient-phytoplankton model with instantaneous nutrient recycling, where we use an uptake function which is a generalization of those used by many authors. We investigate the dynamical properties of this model by showing the existence of a boundary equilibrium point, and using a geometrical method to find the conditions for the existence of one or two positive equilibrium points. Moreover, geometrical and analytical methods are used to determine the local stability of the different equilibrium points, and a sufficient condition for the global stability of the boundary equilibrium point is given. We also discuss the possibility of the existence of saddle-node or Hopf bifurcations under different conditions.

In chapter 3 we modify the previous model by introducing the delayed nutrient recycling. By investigating the distribution of the roots in the corresponding characteristic equation and discussing the effect of time delay on the stability of the different equilibrium points, sufficient conditions are given, respectively, for the occurrence of stability switches and Hopf-Zero bifurcation.

In chapter 4 we focus on the study of the bifurcations for both the instantaneous and delayed models, where we use the projection method, center manifold theorem and normal form approach to discuss the saddle-node bifurcation for the instantaneous system, Hopf bifurcations can occurfor the systems with or without delay. The Hopf-Zero bifurcation occurs only for the system with delay.

Numerical simulations are given in chapter 5 to illustrate the theoretical predictions provided in the previous chapters. Biological interpretations of these simulations are addressed.

In the last chapter we provide conclusions that summarize the results obtained in this research project, and provide suggestions to improve the model.

Chapter 2

STABILITY ANALYSIS OF THE TWO DIMENSIONAL (N, A) SYSTEM

In this chapter we present the two dimensional mathematical model to describe the interactions between nutrient N and phytoplankton A in Section 1, and investigate the existence of the equilibrium points in Section 2. The stability analysis of these equilibrium points is given in Section 3.

2.1 The Model

Huppert et al [24] have proposed a simple nutrient-phytoplankton model that consists of only two variables; nutrient level N, and phytoplankton biomass A. It assumes that nutrient input flows into the system, and is lost from the system by sedimentation. The phytoplankton A rely on nutrient "uptake" for growth, and is removed from the water column through mortality and sinking. This gives the following system

$$\dot{N} = \text{input - uptake - loss,}$$

$$\dot{A} = \text{uptake - death - sinking.}$$

and they choose nutrient input as a constant and use the bilinear Lotka-Voltera interaction term to describe the nutrient uptake by phytoplankton. Although this model is of a very simple structure, it is useful, and its dynamics is important to more complex nutrient-phytoplankton models.

To make the model more realistic, we modify it by adding the nutrient recycling which gives the following general system

$$\dot{N} = \text{input - loss - uptake + recycling,}$$

$$\dot{A} = \text{uptake - death - sinking.}$$

and we choose the nutrient uptake by phytoplankton as a nonlinear uptake function which is a product of Holling Types II and III functional responses [26], namely $F(N)G(A)A$. It describes how the consumption of nutrients by phytoplankton depends on both densities. $F(N)$ is Holling type II functional response in which the phytoplankton consumption rate rises gradually with nutrient density, until it reaches a relatively constant level at which the consumption rate remains constant irrespective of nutrient density [27]. $G(A)A$ is Holling type III functional response in which $G(A)$ describes how the nutrient biomass is consumed by phytoplankton. It increases first and then decreases with increasing phytoplankton density. Explicit formulas of Holling Types II and III functional responses have been proposed by many authors [28, 29, 30, 31]. More generally, we assume that the functions $F(N)$, $G(A)$ satisfy the following conditions

(C_1) $\quad F' > 0 \;\;,\;\; F'' < 0 \;\;,\;\; F(0) = 0 \;\;,\;\; \lim_{N\to\infty} F(N) = 1.$

(C_2) $\quad G(0) = 0 \;\;,\;\; \lim_{A\to\infty} G(A) = 0$, and there exists a maximum point A^*

such that $G'(A^*) = 0$, $G'(A) > 0$ for all $A < A^*$, $G'(A) < 0$ for all $A > A^*$.

For instance

$$F(N) = \frac{N^p}{N^p + h^p} \qquad (p > 0) \quad , \quad G(A) = \frac{A^{q-1}}{A^q + k^q} \qquad (q > 1).$$

are functions satisfying (C_1) and (C_2) respectively, where h, k are the half saturation constants of nutrient and phytoplankton, respectively. The sample graphs of F and G are given in Figure (2.1).

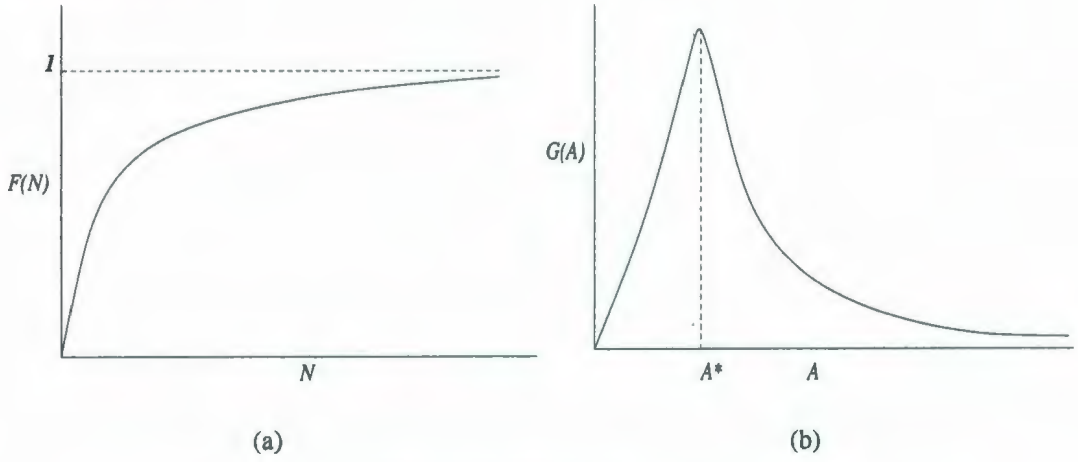

Figure 2.1: The schematic graph of (a) $F(N)$, and (b) $G(A)$.

More specifically we choose the nutrient input as a constant, and assume that the nutrient loss by sedimentation, the nutrient recycling and the phytoplankton mortality are all linear functions, and the nutrient uptake by phytoplankton is represented by the proposed nonlinear uptake function, yielding the following

$$\begin{aligned} \frac{dN}{dt} &= L - sN - rF(N)G(A)A + bA = H_1(N, A), \\ \frac{dA}{dt} &= grF(N)G(A)A - mA = H_2(N, A), \end{aligned} \tag{2.1}$$

where the parameter L represents the rate of N input, s is the rate of N output due to sedimentation, r is the maximum per-capita grazing rate, b is the rate of nutrient recycling of the dead phytoplankton biomass by bacterial decomposition, g is the conversion rate of nutrient into phytoplankton, and m is the phytoplankton mortality rate. All the parameters L, s, r, b, g, and m are positive.

We will analyse the system (2.2) mathematically. First, we have the following result about its solution.

Theorem 2.1.1. *All the solutions in (2.1) are bounded.*

Proof:

From $\frac{dA}{dt} = grF(N)G(A)A - mA \leq (grG(A) - m)A$. Since $\lim_{A\to\infty} G(A) = 0$, there exists A_0 such that when $A > A_0$, $G(A) < \frac{m}{gr}$, i.e, $\frac{dA}{dt} < 0$ for $A > A_0$, hence, there exists M_A such that $A \leq M_A$ for $A > A_0 \Rightarrow A$ is bounded.

From $\frac{dN}{dt} = L - sN - rF(N)G(A)A + bA \leq L + bM_A - sN$, when $N > \frac{L + bM_A}{s} = N_0$, $\frac{dN}{dt} < 0 \Rightarrow N$ is bounded as well.

In the following section we discuss the existence of the equilibrium points of system (2.1).

2.2 The Equilibrium Points

The equilibrium points of (2.1) satisfies $H_1(N, A) = H_2(N, A) = 0$. Obviously, the boundary equilibrium point $E_0 = (\frac{L}{s}, 0)$ always exists.

To discuss the existence of the positive equilibrium points, from (2.1) we work on the

equations

$$F(N)G(A) = \frac{m}{gr}, \tag{2.2}$$

and

$$N = f_1(A) = \frac{1}{s}[L - \frac{m - bg}{g}A]. \tag{2.3}$$

From $F(N) = \frac{m}{gr} \cdot \frac{1}{G(A)}$ and $0 \leq F(N) < 1$, we have $\frac{m}{gr} < G(A)$. Since $G(A) \leq G(A^*)$ from (C_2), if the positive equilibrium points exists in (2.2),(2.3) then the parameters m, g, r satisfy $\frac{m}{gr} < G(A^*)$, therefore, the values of A which satisfy Eq. (2.2) must fit the inequality $\frac{m}{gr} < G(A) < G(A^*)$.

Due to the continuity of $G(A)$, it is obvious that there exists $0 < A_1 < A^* < A_2$ such that

$$G(A_1) = G(A_2) = \frac{m}{gr},$$

The solution of (2.2) satisfies $A_1 < A < A_2$. Moreover, from $F(N) = \frac{m}{gr} \cdot \frac{1}{G(A)} = f(A)$, we have $N = F^{-1}(f(A)) = f_2(A)$. Since $f(A_1) = f(A_2) = 1$, and $\lim_{N\to\infty} F(N) = 1$,

$$\Longrightarrow \quad \lim_{A\to A_1} f_2(A) = +\infty, \quad \lim_{A\to A_2} f_2(A) = +\infty.$$

From $f'(A) = -\frac{m}{gr}\frac{G'(A)}{G^2(A)} = \begin{cases} < 0 \quad if \quad A_1 < A < A^*, \\ = 0 \quad if \quad A = A^*, \\ > 0 \quad if \quad A^* < A < A_2, \end{cases}$ by the assumption (C_2),

and

$$f_2'(A) = \frac{dF^{-1}(f(A))}{dA} = \frac{dF^{-1}(f(A))}{df(A)} \cdot \frac{df(A)}{dA},$$

we have

$$f_2'(A) = \begin{cases} < 0 & if \quad A_1 < A < A^*, \\ = 0 & if \quad A = A^*, \\ > 0 & if \quad A^* < A < A_2, \end{cases}$$

since $\dfrac{dF^{-1}(f(A))}{df(A)} > 0$ due to the monotonic property of the function F.

The previous facts suggest that the graph of the function $f_2(A)$ is as follows

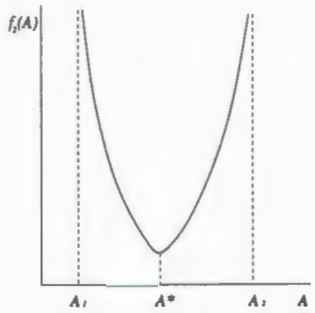

Figure 2.2: The schematic graph of $f_2(A)$.

Therefore, geometrically, the positive equilibrium points are the intersection points of the two curves $f_1(A)$ and $f_2(A)$ which suggests that there exists at most two positive equilibrium points. See Figure (2.3).

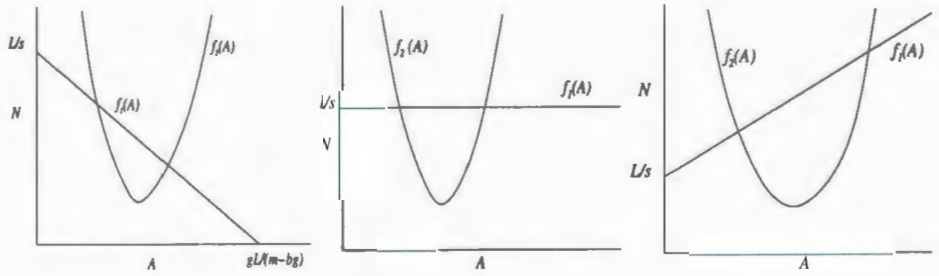

(a) (b) (c)

Figure 2.3: The schematic graphs of $f_1(A)$, $f_2(A)$ (a) $m > bg$, (b) $m = bg$, (c) $m < bg$.

Although we can observe the possible existence of positive equilibrium points from Figure (2.3), to find the conditions under which the system has none, one or two positive equilibrium points, and further to discuss their stabilities, we need to solve the two Eqs. (2.2) and (2.3) simultaneously. Substituting (2.3) into (2.2) gives the equation

$$F\{\frac{1}{s}[L - \frac{m - bg}{g}A]\} \cdot G(A) = \frac{m}{gr}. \tag{2.4}$$

Let the function in the left-hand side of (2.4) be $H(A)$

$$H(A) = F\{\frac{1}{s}[L - \frac{m - bg}{g}A]\} \cdot G(A).$$

It is easy to see that $H(A) \geq 0$, $H(0) = 0$. Obviously, when $m > bg$ the domain of $H(A)$ is $0 \leq A \leq \frac{gL}{m - bg}$ and $H(\frac{gL}{m - bg}) = 0$, while when $m \leq bg$ the domain of $H(A)$ is $A \geq 0$ and $\lim_{A \to \infty} H(A) = 0$. Also

$$H'(A) = -\frac{m - bg}{gs}F'\{\frac{1}{s}[L - \frac{m - bg}{g}A]\} \cdot G(A) + F\{\frac{1}{s}[L - \frac{m - bg}{g}A]\} \cdot G'(A) \tag{2.5}$$

We have the following Lemma about the sign of $H'(A)$.

Lemma 2.2.1. *There exists $\hat{A}$ such that,*

$$(1)H'(A) = \begin{cases} > 0 & if \quad A < \hat{A}, \\ = 0 & if \quad A = \hat{A}, \\ < 0 & if \quad A > \hat{A}. \end{cases} \quad \textit{Moreover,} \quad (2)\hat{A} = \begin{cases} < A^* & if \quad m > bg, \\ = A^* & if \quad m = bg, \\ > A^* & if \quad m < bg. \end{cases}$$

Proof:

First we consider the case $m > bg$. Since $F > 0$, $F' > 0$, $G > 0$, there exists $\hat{A}$ such that $G'(\hat{A}) > 0$ and satisfies $H'(\hat{A}) = 0$ in (2.5). In addition, we can locate $\hat{A} < A^*$ from

(2.1). $f_1(A) = \frac{1}{s}[L - \frac{m-bg}{g}A]$ is a decreasing function, and $F' > 0, F'' < 0$. By noticing the domain of $H(A)$ for $m > bg$ is $[0, \frac{gL}{m-bg}]$, we have the following

i) when $A < \hat{A} < A^*$,

$$\frac{1}{s}[L - \frac{m-bg}{g}A] > \frac{1}{s}[L - \frac{m-bg}{g}\hat{A}],$$

$$F(\frac{1}{s}[L - \frac{m-bg}{g}A]) > F(\frac{1}{s}[L - \frac{m-bg}{g}\hat{A}]) \geq 0,$$

$$0 < F'(\frac{1}{s}[L - \frac{m-bg}{g}A]) < F'(\frac{1}{s}[L - \frac{m-bg}{g}\hat{A}]),$$

$$0 \leq G(A) < G(\hat{A}) \quad , \quad G'(A) > G'(\hat{A}) > 0.$$

Consequently in (2.5)

$$H'(A) > -\frac{m-bg}{gs}F'(\frac{1}{s}[L-\frac{m-bg}{g}\hat{A}])G(\hat{A})+F(\frac{1}{s}[L-\frac{m-bg}{g}\hat{A}])G'(\hat{A}) = H'(\hat{A}) = 0.$$

ii) when $\hat{A} < A < A^*$,

$$\frac{1}{s}[L - \frac{m-bg}{g}A] < \frac{1}{s}[L - \frac{m-bg}{g}\hat{A}],$$

$$0 < F(\frac{1}{s}[L - \frac{m-bg}{g}A]) < F(\frac{1}{s}[L - \frac{m-bg}{g}\hat{A}]),$$

$$F'(\frac{1}{s}[L - \frac{m-bg}{g}A]) > F'(\frac{1}{s}[L - \frac{m-bg}{g}\hat{A}]) > 0,$$

$$G(A) > G(\hat{A}) \geq 0 \quad , \quad 0 < G'(A) < G'(\hat{A}),$$

hence,

$$H'(A) < -\frac{m-bg}{gs}F'(\frac{1}{s}[L-\frac{m-bg}{g}\hat{A}])G(\hat{A})+F(\frac{1}{s}[L-\frac{m-bg}{g}\hat{A}])G'(\hat{A}) = H'(A) = 0.$$

iii) when $A^* \leq A \leq \frac{gL}{m-bg}$,

$$\frac{1}{s}[L - \frac{m-bg}{g}A] \leq \frac{1}{s}[L - \frac{m-bg}{g}A^*],$$

$$0 \leq F(\frac{1}{s}[L - \frac{m-bg}{g}A]) \leq F(\frac{1}{s}[L - \frac{m-bg}{g}A^*]),$$

$$F'(\frac{1}{s}[L - \frac{m-bg}{g}A]) \geq F'(\frac{1}{s}[L - \frac{m-bg}{g}A^*]) > 0,$$

$$0 < G(A) \leq G(A^*) \quad , \quad G'(A) \leq G'(A^*) = 0,$$

consequently

$$H'(A) < -\frac{m-bg}{gs}F'(\frac{1}{s}[L - \frac{m-bg}{g}A^*])G(A^*) + F(\frac{1}{s}[L - \frac{m-bg}{g}A^*])G'(A^*) < 0.$$

therefore, for any $A \in [0, \frac{gL}{m-bg}]$ the results (1) and (2) hold. Similarly we can prove the results when $m \leq bg$.

The previous facts suggest that the function $H(A)$ has the following shape, Figure (2.4).

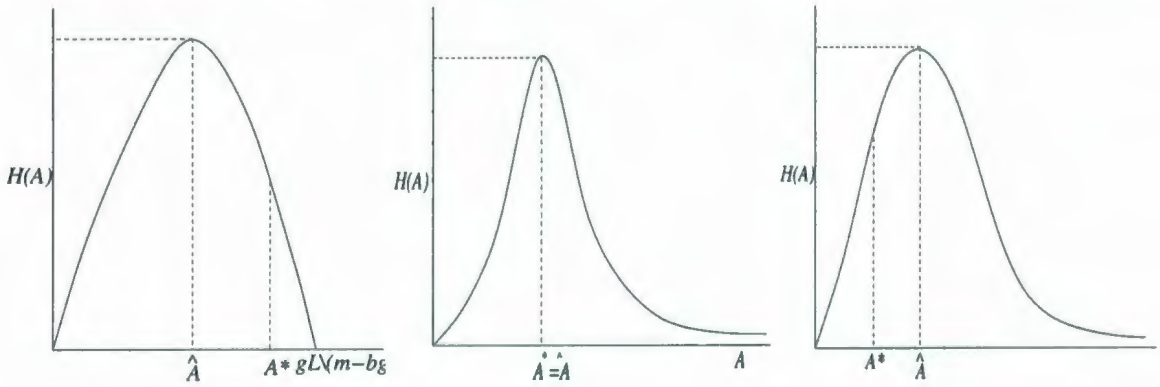

(a) (b) (c)

Figure 2.4: The schematic graph of $H(A)$ (a) $m > bg$, (b) $m = bg$, (c) $m < bg$.

The roots of Eq.(2.4), (i.e; $H(A) = \frac{m}{gr}$) are the intersections between the graph of the function $H(A)$ and the horizontal line $\frac{m}{gr}$. In the following we determine the different cases in which Eq.(2.4) has none, one or two positive roots. Furthermore, we determine the

location of each positive root with respect to $\hat{A}$ and A^*, since we will need this information in Section 3 to determine the stability of the corresponding equilibrium points.

Case 0: $H(\hat{A}) < \frac{m}{gr}$ (Figure (2.5)). Since there is no intersection between the graph of $H(A)$ and the horizontal line $\frac{m}{gr}$, hence Eq.(2.4) has no positive root.

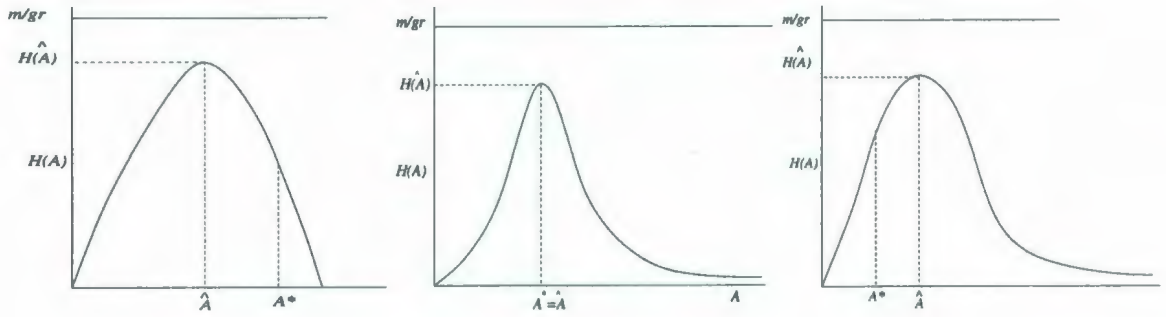

(a) (b) (c)

Figure 2.5: Case 0 $H(\hat{A}) < \frac{m}{gr}$ (a) $m > bg$, (b) $m = bg$, (c) $m < bg$.

Case 1: $H(\hat{A}) = \frac{m}{gr}$ (Figure (2.6)). The horizontal line $\frac{m}{gr}$ is tangent to the curve of $H(A)$ at the point $(\hat{A}, H(\hat{A}))$, implies Eq.(2.4) has one positive root A_1^* satisfying $A_1^* = \hat{A} < (\geq) A^*$ when $m > (\leq) bg$.

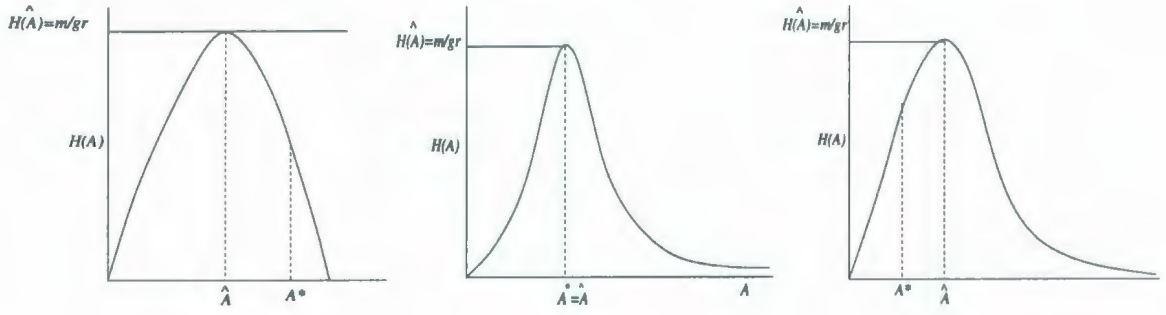

(a) (b) (c)

Figure 2.6: Case 1 $H(\hat{A}) = \frac{m}{gr}$ (a) $m > bg$, (b) $m = bg$, (c) $m < bg$.

Case 2: $H(A^*) < \frac{m}{gr} < H(\hat{A})$ $(m \neq bg)$(Figure (2.7)). There are two intersection points between the graph of $H(A)$ and the horizontal line $\frac{m}{gr}$, and hence Eq.(2.4) has two positive roots A_1^* and A_2^* satisfying $A_1^* < \hat{A} < A_2^* < A^*$ when $m > bg$, and $A^* < A_1^* < \hat{A} < A_2^*$ when $m < bg$.

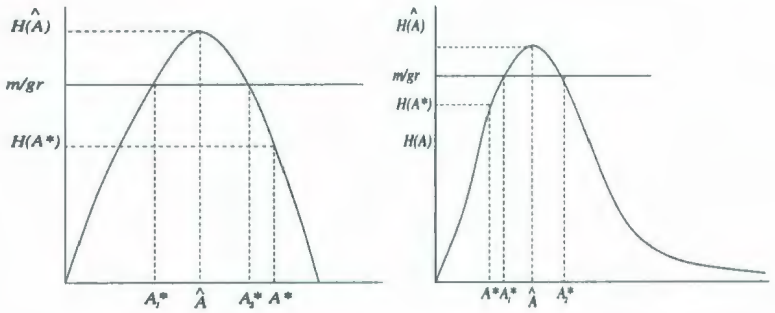

(a) (b)

Figure 2.7: Case 2 $H(A^*) < \frac{m}{gr} < H(\hat{A})$ (a) $m > bg$, (b) $m < bg$.

Case 3: $H(A^*) \geq \frac{m}{gr}$ (Figure (2.8)). There are two intersection points A_1^* and A_2^* as well. Where $A_1^* < \hat{A} < A^* \leq A_2^*$ when $m > bg$, $A_1^* < A^* = \hat{A} < A_2^*$ when $m = bg$, and $A_1^* \leq A^* < \hat{A} < A_2^*$ when $m < bg$.

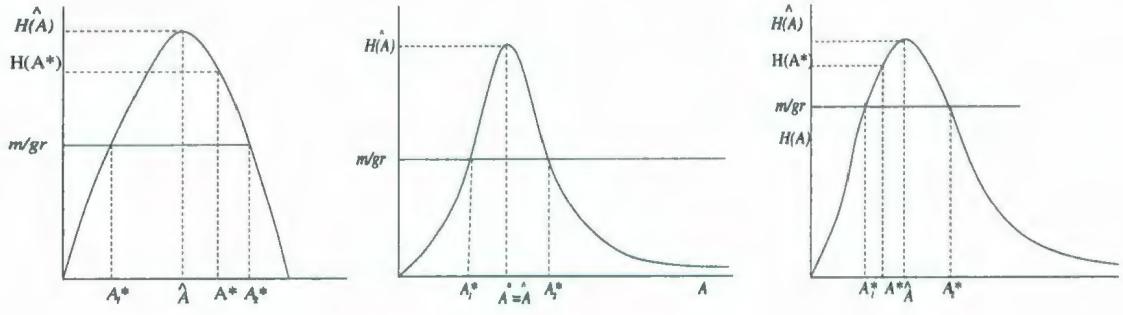

(a) (b) (c)

Figure 2.8: Case 3 $H(A^*) \geq \frac{m}{gr}$ (a) $m > bg$, (b) $m = bg$, (c) $m < bg$.

The following table summarizes the conditions for the existence of roots in (2.4)

Case #	Condition	Roots of Eq.(2.5)
0	$H(\hat{A}) < \frac{m}{gr}$	No positive roots exist
1	$H(\hat{A}) = \frac{m}{gr}, m > bg$	$A_1^* = \hat{A} < A^*$
	$H(\hat{A}) = \frac{m}{gr}, m = bg$	$A_1^* = \hat{A} = A^*$
	$H(\hat{A}) = \frac{m}{gr}, m < bg$	$A_1^* = \hat{A} > A^*$
2	$H(A^*) < \frac{m}{gr} < H(\hat{A}), m > bg$	$A_1^* < \hat{A} < A_2^* < A^*$
	$H(A^*) < \frac{m}{gr} < H(\hat{A}), m < bg$	$A^* < A_1^* < \hat{A} < A_2^*$
3	$H(A^*) \geq \frac{m}{gr}, m > bg$	$A_1^* < \hat{A} < A^* \leq A_2^*$
	$H(A^*) \geq \frac{m}{gr}, m = bg$	$A_1^* < A^* = \hat{A} < A_2^*$
	$H(A^*) \geq \frac{m}{gr}, m < bg$	$A_1^* \leq A^* < \hat{A} < A_2^*$

Table 2.1

After obtaining the values of A_1^* and A_2^*, the corresponding values of N_1^* and N_2^* can be determined by Eq.(2.4). Therefore, we can obtain the positive equilibrium points in (2.1) denoted by $E_1 = (N_1^*, A_1^*)$ and $E_2 = (N_2^*, A_2^*)$.

In the following section we determine the stability type of each equilibrium point in each case.

2.3 Stability Analysis

The local stability of an equilibrium point can be determined by calculating the eigenvalues of the Jacobian matrix at this point. For the two dimensional system (2.2), if the two eigen-

values have negative real parts then the corresponding equilibrium point is locally asymptotically stable. If at least one eigenvalue has a positive real part then the corresponding equilibrium point is unstable.

The Jacobian matrix of system (2.1) is

$$J(N,A) = \begin{pmatrix} \frac{\partial H_1}{\partial N} & \frac{\partial H_1}{\partial A} \\ \frac{\partial H_2}{\partial N} & \frac{\partial H_2}{\partial A} \end{pmatrix}$$

$$= \begin{pmatrix} -s - rF'(N)G(A)A & -rF(N)G'(A)A - rF(N)G(A) + b \\ grF'(N)G(A)A & grF(N)G'(A)A + grF(N)G(A) - m \end{pmatrix}$$

Case 0: (There is no positive equilibrium point)(See Figure (2.5)).

In this case the only equilibrium point is the boundary equilibrium point $E_0 = (\frac{L}{s}, 0)$. The Jacobian matrix at this point is

$$J(\frac{L}{s}, 0) = \begin{pmatrix} -s & b \\ 0 & -m \end{pmatrix}$$

and so the two eigenvalues are $\lambda_1 = -s < 0$, $\lambda_2 = -m < 0$. Hence E_0 is always locally asymptotically stable.

Moreover, under certain condition, E_0 can be globally asymptotically stable.

Theorem 2.3.1. *If $G(A^*) \leq \frac{m}{gr}$, then the boundry equilibrium point E_0 is globally asymptotically stable in $R^2_+ = \{(N,A) \in R^2 : N > 0, A \geq 0\}$.*

Proof:

From $G(A) \leq G(A^*)$, $0 \leq F(N) < 1$ we have

$$\frac{dA}{dt} = grF(N)G(A)A - mA < grG(A^*)A - mA = (grG(A^*) - m)A$$

Since $G(A^*) \leq \frac{m}{gr}$, $\frac{dA}{dt} < 0$, and $\lim_{t\to\infty} A(t) = 0$. Substituting $A = 0$ into (2.2) gives $N' = L - sN \Longrightarrow N(t) = \frac{L}{s} + ce^{-st}$, therefore $\lim_{t\to\infty} N(t) = \frac{L}{s}$, implying that E_0 is globally asymptotically stable.

Remark 2.3.1. When $H(\hat{A}) < \frac{m}{gr} < G(A^*)$, there are no positive equilibrium points (See Figure (2.5)). The boundary equilibrium point E_0 is the unique equilibrium point. We can conject that E_0 is also globally asymptotically stable, although we can't prove it rigorously. However, numerical simulation can support this conjecture. We choose $F(N) = \frac{N}{N+1}$, $G(A) = \frac{A}{A^2+1}$, $L = 0.2$, $s = 0.05$, $b = 0.15$, $g = 1$, $m = 0.24$, and $r = 0.6$. Then $H(\hat{A}) = 0.35 < \frac{m}{gr} = 0.4 < G(A^*) = 0.5$. The phase portrait (Figure (2.9)) illustrates the global stability of the boundary equilibrium point.

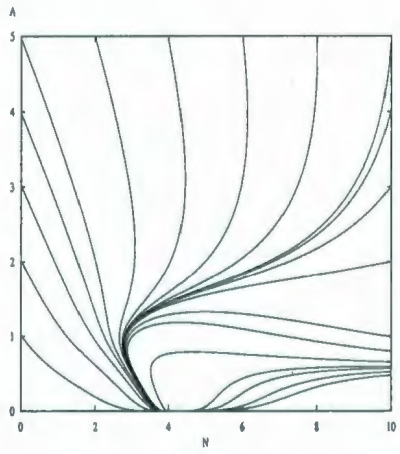

Figure 2.9: The phase portrait of system (2.2).

In the following we study the local stability of the positive equilibrium points in Cases 1,2 and 3.

The positive equilibrium points $E_1 = (N_1^*, A_1^*)$, $E_2 = (N_2^*, A_2^*)$ satisfy

$$F(N_i^*)G(A_i^*) = \frac{m}{gr}. \quad (i = 1, 2).$$

The Jacobian matrix at each equilibrium point is

$$J(N_i^*, A_i^*) = \begin{pmatrix} -s - rF'(N_i^*)G(A_i^*)A_i^* & -rF(N_i^*)G'(A_i^*)A_i^* - \frac{m}{g} + b \\ grF'(N_i^*)G(A_i^*)A_i^* & grF(N_i^*)G'(A_i^*)A_i^* \end{pmatrix}$$

Let $K_i^1 = F'(N_i^*)G(A_i^*)A_i^*$, $K_i^2 = F(N_i^*)G'(A_i^*)A_i^*$,

$$J(N_i^*, A_i^*) = \begin{pmatrix} -s - rK_i^1 & -rK_i^2 - \frac{m}{g} + b \\ grK_i^1 & grK_i^2 \end{pmatrix}$$

$$detJ = -sgrK_i^2 + rK_i^1(m - bg) \ , \ TrJ = -s - rK_i^1 + grK_i^2$$

Lemma 2.3.2. *If* $A_i^* < (\geq \hat{A})$ *then* $detJ < (\geq)0$.

Proof:

It is easy to see that $K_i^1 > 0$. When $A_i^* < (\geq \hat{A})$, $H'(A_i^*) > (\leq 0)$ (from Lemma 2.2.1).

$$\begin{aligned} A_i^* H'(A_i^*) &= -\frac{m - bg}{gs} F'(N_i^*)G(A_i^*)A_i^* + F(N_i^*)G'(A_i^*)A_i^*, \\ &= -\frac{m - bg}{gs} K_i^1 + K_i^2, \\ &= \frac{1}{gs}[gsK_i^2 - (m - bg)K_i^1], \\ &= -\frac{1}{gsr} detJ\Big|_{A_i^*} > (\leq 0). \end{aligned}$$

therefore $detJ\Big|_{A_i^*} < (\geq 0)$ for $A_i^* < (\geq \hat{A})$.

It is noted that when $A_i^* < (\geq)A^*$, $G'(A_i^*) > (\leq)0$ (from (2.1)), so $K_i^2 > (\leq)0$. Moreover, if $K_i^2 \leq 0$, $TrJ < 0$ is obvious, while when $K_i^2 > 0$, then the sign of TrJ is changeable.

Combining the information given in Table 2.1, the stability type of the positive equilibrium points in Cases 1,2 and 3 can be determined as follows

Case 1: (There exists only one positive equilibrium point $E_1 = (N_1^*, A_1^*) = (\hat{N}, \hat{A})$)(See Figure (2.6)).

1) When $m > bg$, $A_1^* = \hat{A} < A^*$, $detJ = 0$ and $K_1^2 > 0$, hence,

if $K_1^2 < \dfrac{s + rK_1^1}{gr}$, then $TrJ < 0$, the eigenvalues are $\lambda_1 = 0, \lambda_2 < 0$, that means E_1 is a degenerate stable equilibrium point;

if $K_1^2 = \dfrac{s + rK_1^1}{gr}$, then $TrJ = 0$, the eigenvalues are $\lambda_1 = \lambda_2 = 0$, that means E_1 is a degenerate equilibrium point, and we can not determine the stability from the linearized system;

if $K_1^2 > \dfrac{s + rK_1^1}{gr}$, then $TrJ > 0$, the eigenvalues are $\lambda_1 = 0, \lambda_2 > 0$, that means E_1 is an unstable equilibrium point. Therefore, when $K_1^2 = \dfrac{s + rK_1^1}{gr}$, there is a steady-state bifurcation.

2) When $m \leq bg$,$A_1^* = \hat{A} \geq A^*$, $detJ = 0$ and $TrJ < 0$ since $K_1^2 \leq 0$, the eigenvalues are $\lambda_1 = 0, \lambda_2 < 0$, that means E_1 is a degenerate stable equilibrium point.

Case 2: (There exists two positive equilibrium points $E_1 = (N_1^*, A_1^*), E_2 = (N_2^*, A_2^*)$)(See Figure (2.7)).

1) When $m > bg$, $A_1^* < \hat{A} < A_2^* < A^*$, $detJ\Big|_{A_1^*} < 0$, so E_1 is a saddle point. Also, $detJ\Big|_{A_2^*} > 0$ and $K_2^2 > 0$, hence,

if $K_2^2 < \dfrac{s + rK_2^1}{gr}$, then $TrJ\Big|_{A_2^*} < 0$, the eigenvalues are $\lambda_1 < 0, \lambda_2 < 0$, then E_2 is locally asymptotically stable equilibrium point.

If $K_2^2 = \dfrac{s + rK_2^1}{gr}$, then $TrJ\Big|_{A_2^*} = 0$. The eigenvalues are $\lambda_{1,2} = \pm i\omega$. Then there is a

possibility of the existence of a Hopf bifurcation.

If $K_2^2 > \dfrac{s+rK_2^1}{gr}$, then $TrJ\Big|_{A_2^*} > 0$. The eigenvalues are $\lambda_1 > 0, \lambda_2 > 0$. Then E_2 is an unstable equilibrium point.

2) When $m < bg$, $A^* < A_1^* < \hat{A} < A_2^*$, $detJ\Big|_{A_1^*} < 0$ and $TrJ\Big|_{A_1^*} < 0$, E_1 is a saddle point. While $detJ\Big|_{A_2^*} > 0$ and $TrJ\Big|_{A_2^*} < 0$, hence, E_2 is locally asymptotically stable.

Case 3: (There exist two positive equilibrium points $E_1 = (N_1^*, A_1^*), E_2 = (N_2^*, A_2^*)$)(See Figure (2.8)).

Similarly, by determining the signs of $detJ$ and TrJ at each E_i $(i = 1, 2)$ we know E_1 is a saddle point and E_2 is locally asymptotically stable.

Therefore, the stability of the positive equilibrium points in the different cases is summarized as following

Case #	Condition	$K_i^2 < \frac{s+rK_i^1}{gr}$	$K_i^2 = \frac{s+rK_i^1}{gr}$	$K_i^2 > \frac{s+rK_i^1}{gr}$
1	$H(\hat{A}) = \frac{m}{gr}, m > bg$	E_1 is degenerate stable	E_1 is degenerate	E_1 unstable
	$H(\hat{A}) = \frac{m}{gr}, m \leq bg$	$E_1$is degenerate stable	—	—
2	$H(A^*) < \frac{m}{gr} < H(\hat{A}), m > bg$	E_1 saddle E_2 asymptotically stable (AS)	E_1 saddle E_2 :there is a possibility of the existence of a Hopf bifurcation	E_1 saddle E_2 unstable
	$H(A^*) < \frac{m}{gr} < H(\hat{A}), m < bg$	E_1 saddle E_2 AS	— —	— —
3	$H(A^*) \geq \frac{m}{gr}$	E_1 saddle E_2 AS	E_1 saddle —	E_1 saddle —

Table 2.2

Where "—" means does not exist.

Chapter 3

STABILITY ANALYSIS OF THE TWO DIMENSIONAL (N, A) SYSTEM WITH TIME DELAY τ

There is a time required to regenerate nutrient from dead phytoplankton biomass by bacterial decomposition. Such a delay is always present in natural systems and increases with decreasing temperature [32]. Therefore, it is necessary to study the nutrient-phytoplankton system (2.2) with delayed nutrient recycling, and to discuss the effects of introducing this time delay on the stability of its equilibrium points.

Consider the following (N, A) model with time delay τ

$$\begin{aligned} \frac{dN}{dt} &= L - sN - rF(N)G(A)A + bA(t-\tau), \\ \frac{dA}{dt} &= grF(N)G(A)A - mA. \end{aligned} \tag{3.1}$$

this system has the same equilibrium points as system (2.2) under the same conditions.

3.1 Stability Analysis

First, we consider the stability of the boundary equilibrium point $E_0 = (\frac{L}{s}, 0)$.
The following transformation of variables $x = N - \frac{L}{s}$ and $y = A$ transforms E_0 to the trivial equilibrium point $(0, 0)$, and gives

$$F(N) = F(x + \frac{L}{s}) = F(\frac{L}{s}) + xF'(\frac{L}{s}) + O(x^2),$$
$$G(A) = G(y) = G(0) + yG'(0) + O(y^2) = yG'(0) + O(y^2). \tag{3.2}$$

Substituting (3.2) into the model (3.1) yields the following system

$$\begin{aligned} \dot{x} &= -sx + by(t-\tau) + O(x^2 + y^2), \\ \dot{y} &= -my + O(x^2 + y^2). \end{aligned} \tag{3.3}$$

The characteristic matrix at the trivial solution $(0, 0)$ is

$$\triangle(\lambda) = \begin{pmatrix} \lambda + s & -be^{-\lambda\tau} \\ 0 & \lambda + m \end{pmatrix}$$

which has two eigenvalues $\lambda_1 = -s < 0, \lambda_2 = -m < 0$, implying that $(0, 0)$ is always locally asymptotically stable for any $\tau \geq 0$, this indicates that the time delay τ does not affect the stability of the boundary equilibrium point E_0.

Now we study the stability of the positive equilibrium point $(\tilde{N}, \tilde{A})$.
Let $x = N - \tilde{N}$ and $y = A - \tilde{A}$ then model (3.1) becomes

$$\begin{aligned} \dot{x} &= -x(s + rF'(\tilde{N})G(\tilde{A})\tilde{A})) - y(\frac{m}{g} + rF(\tilde{N})G'(\tilde{A})\tilde{A}) + by(t-\tau) + O(x^2 + y^2). \\ \dot{y} &= grF'(\tilde{N})G(\tilde{A})\tilde{A}x + grF(\tilde{N})G'(\tilde{A})\tilde{A}y + O(x^2 + y^2). \end{aligned} \tag{3.4}$$

Let $K^1 = F'(\tilde{N})G(\tilde{A})\tilde{A}$, $K^2 = F(\tilde{N})G'(\tilde{A})\tilde{A}$, the characteristic matrix at the origin is

$$\triangle(\lambda) = \begin{pmatrix} \lambda + s + rK^1 & \frac{m}{g} + rK^2 - be^{-\lambda\tau} \\ -grK^1 & \lambda - grK^2 \end{pmatrix}$$

then the characteristic equation is

$$\begin{aligned} \ell(\lambda,\tau) &\triangleq \lambda^2 + (s + rK^1 - grK^2)\lambda + rK^1 m - sgrK^2 - grK^1 be^{-\lambda\tau} \\ &= \lambda^2 + \alpha\lambda + \beta + \gamma e^{-\lambda\tau} = 0 \end{aligned} \tag{3.5}$$

where $\alpha = s + rK^1 - grK^2$, $\beta = rK^1 m - sgrK^2$, $\gamma = -grK^1 b < 0$.

Since (3.4) is an infinite dimensional system, (3.5) is usually transcendental, hence, the distribution of the roots in (3.5) is usually more complicated than that for the finite dimensional system without delay. The following Lemma investigates the distribution of the roots in (3.5).

Lemma 3.1.1.

In E.q (3.5)

1) If $(H_{11}) : \beta + \gamma > 0$ *and* $(H_{12}) : \alpha \geq \sqrt{2\beta}$, *then all the roots have negative real parts.*

If $(H_{21}) : \beta + \gamma = 0$, *and* $\tau \leq \frac{\alpha}{\gamma}$, $\alpha < 0$, *then there exists a zero root and all other roots have negative real parts.*

If $(H_{31}) : \beta + \gamma < 0$ *or* $(H_{32}) : \beta + \gamma = 0$, *and* $\tau > \frac{\alpha}{\gamma}$, $\alpha < 0$, *then there exists at least one root with positive real part.*

2) If $(H_{41}) : |\beta| < -\gamma$, *then there exists one pair of purely imaginary roots* $\lambda = \pm i\omega_+$, *at a sequence of critical values of* τ.

If $(H_{51}) : \beta = -\gamma > \frac{\alpha^2}{2}$, *then there exists a zero root and one pair of purely*

imaginary roots $\lambda = \pm i\omega_+$, *at a sequence of critical values of* τ.

If $(H_{61}) : \beta > max\{-\gamma, \frac{\alpha^2}{2}\}$, *and* $(H_{62}) : (\alpha^2 - 2\beta)^2 > 4(\beta^2 - \gamma^2)$, *then there exists two pairs of purely imaginary roots* $\lambda_\pm = \pm i\omega_\pm$ *with* $\omega_+ > \omega_- > 0$, *at two sequences of critical values of* τ.

Proof:

1) It is easy to check that when $\beta + \gamma > 0$, $\lambda = 0$ is not a root of Eq. (3.5).

Substituting $\lambda = u + iv$ into (3.5) yields

$$(u + iv)^2 + \alpha(u + iv) + \beta + \gamma e^{-(u+iv)\tau} = 0.$$

Expanding the last equation and equating the real and imaginary parts to zero gives

$$u^2 - v^2 + \alpha u + \beta + \gamma e^{-u\tau} cos v\tau = 0, 2uv + \alpha v - \gamma e^{-u\tau} sin v\tau = 0$$

therefore

$$(u^2 - v^2 + \alpha u + \beta)^2 + (2uv + \alpha v)^2 = \gamma^2 e^{-2u\tau}$$

$e^{-2u\tau} < 1$ for $u > 0$, then $\gamma^2 e^{-2u\tau} < \gamma^2$ and the last equation gives

$$(u^2 - v^2)^2 + 4u^2v^2 + 2\alpha u(u^2 + v^2) + (\alpha^2 + 2\beta)u^2 + (\alpha^2 - 2\beta)v^2 + 2\alpha u\beta + \beta^2 - \gamma^2 < 0. \quad (3.6)$$

Since $\gamma < 0$, so from $\beta + \gamma > 0$, we have $\beta > 0$ and $\beta^2 - \gamma^2 > 0$, so, if $u > 0$ and $\alpha \geq \sqrt{2\beta}$, (3.6) is impossible. Hence, we know that under assumptions (H_{11}) and (H_{12}) all roots in Eq.(3.5) have negative real parts.

From assumption (H_{21}), since $\beta + \gamma = 0$, then

$$\ell(0,\tau) = \beta + \gamma = 0.$$

so $\lambda = 0$ is a root of Eq.(3.5).

Moreover,

$$\left.\frac{\partial \ell(\lambda,\tau)}{\partial \lambda}\right|_{\lambda=0} = \left.(2\lambda + \alpha - \tau\gamma e^{-\lambda\tau})\right|_{\lambda=0} = \alpha - \tau\gamma \geq 0 \text{ if } (H_{21}) \text{ holds.}$$

In addition,

$$\lim_{\lambda\to\infty} \ell(\lambda,\tau) = +\infty,$$

therefore, all the roots of Eq.(3.5) except zero have negative real parts.

Similarly, from assumptions (H_{31}) or (H_{32}), we have

$$\ell(0,\tau) = \beta + \gamma \leq 0, \left.\frac{\partial \ell(\lambda,\tau)}{\partial \lambda}\right|_{\lambda=0} = \alpha - \tau\gamma < 0, \text{ and } \lim_{\lambda\to\infty} \ell(\lambda,\tau) = +\infty.$$

Therefore, there exists $\lambda_0 > 0$ such that $\ell(\lambda_0,\tau) = 0$, i.e, Eq.(3.5) has at least one positive root.

2) Substituting $\lambda = i\omega$ into Eq.(3.5) gives

$$-\omega^2 + \alpha\omega i + \beta + \gamma(cos\omega\tau - isin\omega\tau) = 0.$$

Separating the real and imaginary parts gives the following two equations

$$\begin{aligned} \gamma cos\omega\tau &= \omega^2 - \beta, \\ \gamma sin\omega\tau &= \alpha\omega, \end{aligned} \tag{3.7}$$

which yields

$$(\omega^2 - \beta)^2 + \alpha^2\omega^2 = \gamma^2, \tag{3.8}$$

that is,

$$\omega^4 + (\alpha^2 - 2\beta)\omega^2 + \beta^2 - \gamma^2 = 0.$$

Solving the above equation gives,

$$\omega_{\pm}^2 = \frac{(2\beta - \alpha^2) \pm \sqrt{(\alpha^2 - 2\beta)^2 - 4(\beta^2 - \gamma^2)}}{2}. \tag{3.9}$$

If $\beta^2 < \gamma^2$ (i.e.,$|\beta| < -\gamma$), then Eq. (3.9) determines only one $\omega_+ > 0$. From (3.7) we can determine a sequence of critical values of time delay τ corresponding to ω_+

$$\tau_{n,1} = \frac{\theta_1 + 2\pi n}{\omega_+}$$

where $0 \leq \theta_1 < 2\pi$, $n = 0, 1, 2, ..$ and $cos\theta_1 = \frac{{\omega_+}^2 - \beta}{\gamma}$, $sin\theta_1 = \frac{\alpha\omega_+}{\gamma}$.

If $\beta = -\gamma > \frac{\alpha^2}{2}$ then $\lambda = 0$ is a root of (3.5) and Eq.(3.9) determines only one $\omega_+ > 0$, at the sequence of the critical values of the time delay $\tau_{n,1}$.

When $\beta^2 > \gamma^2$ (i.e.,$|\beta| > -\gamma$), $2\beta > \alpha^2$, which are equivalent to $\beta > max\{-\gamma, \frac{\alpha^2}{2}\}$, and if, in addition $(\alpha^2 - 2\beta)^2 > 4(\beta^2 - \gamma^2)$ then both $\omega_\pm$ in Eq.(3.9) are positive, at two sequences of critical values of τ given by $\tau_{n,1}$ and $\tau_{n,2}$ where

$$\tau_{n,2} = \frac{\theta_2 + 2\pi n}{\omega_-}$$

where $0 \leq \theta_2 < 2\pi$, $n = 0, 1, 2, ...$ and $cos\theta_2 = \frac{{\omega_-}^2 - \beta}{\gamma}$, $sin\theta_2 = \frac{\alpha\omega_-}{\gamma}$.

The proof of Lemma 3.1.1 is completed.

To see the variation of $Re(\lambda(\tau))$ with the change of τ near the purely imaginary eigenvalues we check the sign of $\left.\frac{dRe\lambda(\tau)}{d\tau}\right|_{\lambda=i\omega_\pm}$.

Differentiating the characteristic equation (3.5) with respect to τ gives

$$(2\lambda + \alpha - \tau\gamma e^{-\lambda\tau})\frac{d\lambda(\tau)}{d\tau} = \lambda\gamma e^{-\lambda\tau} \tag{3.10}$$

Hence,

$$(\frac{d\lambda}{d\tau})^{-1} = \frac{(2\lambda+\alpha)e^{\lambda\tau} - \tau\gamma}{\lambda\gamma} = \frac{(2\lambda+\alpha)e^{\lambda\tau}}{\lambda\gamma} - \frac{\tau}{\lambda}.$$

So, $Re(\frac{d\lambda}{d\tau})^{-1}\Big|_{\lambda=i\omega} = \frac{\alpha^2 + 2(\omega^2-\beta)}{\alpha^2\omega^2 + (\omega^2-\beta)^2} = \frac{\pm\sqrt{(\alpha^2-2\beta)^2 - 4(\beta^2-\gamma^2}}{\gamma^2}.$

Therefore

$$\text{sign}\frac{dRe\lambda}{d\tau}\Big|_{\lambda=i\omega} = sign(\pm\sqrt{(\alpha^2-2\beta)^2 - 4(\beta^2-\gamma^2}).$$

i.e.,

$$\frac{dRe\lambda}{d\tau}\Big|_{\lambda=i\omega_+} > 0 \quad , \quad \frac{dRe\lambda}{d\tau}\Big|_{\lambda=i\omega_-} < 0.$$

Consider the function $\tau_n(\omega) = \frac{1}{\omega}(arccos(\frac{\omega^2-\beta}{\gamma} + 2n\pi)$.Then

$$\frac{d\tau_0}{d\omega} = -\frac{1}{\omega^2}arccos(\frac{\omega^2-\beta}{\gamma}) - \frac{2}{\sqrt{\gamma^2-(\omega^2-\beta)^2}} < 0.$$

Since $\omega_+ > \omega_- > 0$, $\tau_{0,1} < \tau_{0,2}$, also $\tau_{n+1,1} - \tau_{n,1} = \frac{2\pi}{\omega_+} < \frac{2\pi}{\omega_-} = \tau_{n+1,2} - \tau_{n,2}$.

Based on the above analysis and Lemma 3.1.1 we have

Theorem 3.1.2.

1) If assumptions (H_{11}) and (H_{12}) are satisfied, then the trivial equilibrium point is locally asymptotically stable for all $\tau > 0$.

2) *If* (H_{21}) *is satisfied, then the trivial equilibrium point undergoes a steady-state bifurcation.*

3) *If* (H_{31}) *is satisfied then the trivial equilibrium point is unstable for any* $\tau > 0$. *If* (H_{32}) *is satisfied, then it is unstable for any* $\tau > \frac{\alpha}{\gamma}$.

4) *Under* (H_{41}),

if the trivial equilibrium point is asymptotically stable for $\tau = 0$, *then it remains asymptotically stable for* $\tau \in (0, \tau_{0,1})$ *and it is unstable for* $\tau > \tau_{0,1}$, *where a Hopf bifurcation occurs at* $\tau = \tau_{0,1}$;

if the trivial equilibrium point is unstable for $\tau = 0$, *then it remains unstable for any* $\tau \geq 0$.

5) *If* (H_{51}) *is satisfied, then the trivial equilibrium point undergoes a Hopf-zero bifurcation at a sequence of critical values of* $\tau_{n,1}$.

6) *If* (H_{61}) *and* (H_{62}) *are satisfied then a stability switch occurs, that is, if the trivial equilibrium point is stable (unstable) for* $\tau = 0$ *then there can be only a finite number of switches between stability (instability) and instability (stability), and there exists a critical value* $\hat{\tau}$ *such that at* $\tau = \hat{\tau}$ *a stability switch occurs from stable to unstable and for* $\tau > \hat{\tau}$ *the solution remains unstable.*

In the following we seek conditions in Lemma 3.1.1 in terms of the parameters s, r, g, m, b in system (3.1) and K^1, K^2 which are related to the equilibrium point $(\tilde{N}, \tilde{A})$.

$(H_{11}) : \beta + \gamma > 0 \Leftrightarrow \dfrac{K^2}{K^1} < \dfrac{m - bg}{gs}$,

$(H_{12}) : \alpha \geq \sqrt{2\beta} \Leftrightarrow s + rK^1 - grK^2 \geq \sqrt{2r(K^1 m - sgK^2)}$, and $K^1 m > sgK^2$,

$(H_{21}) : \beta + \gamma = 0 \Leftrightarrow \frac{K^2}{K^1} = \frac{m - bg}{gs}$ and $\tau \leq \frac{\alpha}{\gamma} \Leftrightarrow \tau \leq \frac{grK^2 - s - rK^1}{grbK^1}$, and

$\alpha < 0 \Longleftrightarrow grK^2 - s - rK^1 > 0,$

$(H_{31}) : \beta + \gamma < 0 \Leftrightarrow \frac{K^2}{K^1} > \frac{m - bg}{gs},$

$(H_{32}) : \beta + \gamma = 0 \Leftrightarrow \frac{K^2}{K^1} = \frac{m - bg}{gs}$ and $\tau > \frac{\alpha}{\gamma} \Leftrightarrow \tau > \frac{grK^2 - s - rK^1}{grbK^1}$, and

$\alpha < 0 \Longleftrightarrow grK^2 - s - rK^1 > 0,$

$(H_{41}) : |\beta| < -\gamma \Leftrightarrow |K^1 m - sgK^2| < gbK^1,$

$(H_{51}) : \beta = -\gamma > \frac{\alpha^2}{2} \Leftrightarrow \frac{K^2}{K^1} = \frac{m - bg}{gs}, \frac{(s + rK^1 - grK^2)^2}{2rgb} < K^1,$

$(H_{61}) : \beta > max\{-\gamma, \frac{\alpha^2}{2}\} \Leftrightarrow K^1 m - sgK^2 > max\{gbK^1, \frac{(s + rK^1 - grK^2)^2}{2r}\},$

$(H_{62}) : (\alpha^2 - 2\beta)^2 > 4(\beta^2 - \gamma^2) \Leftrightarrow \alpha^2(\alpha^2 - 4\beta) + 4\gamma^2 > 0 \Leftrightarrow$

$$(s + rK^1 - grK^2)^2((s + rK^1 - grK^2)^2 - 4r(K^1 m - sgK^2)) + 4g^2 r^2 K^{1^2} b^2 > 0.$$

To discuss the effect of time delay on the stability of the positive equilibrium points, we need to check which assumptions are satisfied for each positive equilibrium point in Cases 1,2 and 3 using the information given in Table (2.2) and Theorem 3.1.2.

Case 1: (There exists only one positive equilibrium point E_1).

At E_1, $\frac{K_1^2}{K_1^1} = \frac{m - bg}{gs}$, i.e, $\beta + \gamma = 0$, it is obvious to see that (H_{21}),(H_{32}), and (H_{51}) are possible.

If (H_{21}) is satisfied, i,e. $K_1^2 > \frac{s + rK_1^1}{gr} (\alpha < 0)$, then E_1 is unstable for $\tau = 0$ and it undergoes a steady state bifurcation for any $\tau \leq \frac{grK_1^2 - s - rK_1^1}{grbK_1^1}$ (Theorem 3.1.2(2)).

If (H_{32}) is satisfied, i,e. $K_1^2 > \frac{s + rK_1^1}{gr} (\alpha < 0)$, then E_1 is unstable for $\tau = 0$ and it remains unstable for any $\tau > \frac{grK_1^2 - s - rK_1^1}{grbK_1^1}$ (Theorem 3.1.2(3)), implying that sufficiently large time delay τ does not affect the stability of E_1.

If (H_{51}) is satisfied, when $\tau = 0$, E_1 is degenerate, and is either stable or unstable. While when $\tau > 0$, there exists a Hopf-Zero bifurcation at a sequence of critical values of $\tau = \tau_{n,1}$ (Theorem 3.1.2(5)).

Case 2: (There exists two positive equilibrium points E_1,E_2).

At E_1, $\frac{K_1^2}{K_1^1} > \frac{m - bg}{gs}$, i.e, $\beta + \gamma < 0$. Obviously, (H_{31}) is satisfied and (H_{41}) is possible. Since E_1 is an unstable (saddle) point when $\tau = 0$, it stays unstable for any $\tau > 0$ under (H_{31}) or (H_{41}) (Theorem 3.1.2(3,4)), implying the time delay τ does not affect its stability.

At E_2, $\frac{K_2^2}{K_2^1} < \frac{m - bg}{gs}$, i.e, $\beta + \gamma > 0$, only (H_{11}) is satisfied. Both (H_{61}) and (H_{62}) are possible.

At $\tau = 0$, if $K_2^2 < \frac{s + rK_2^1}{gr} (\alpha > 0)$, then E_2 is locally asymptotically stable. Hence (H_{12}) is possible. Furthermore, if (H_{12}) holds, then E_2 is also locally asymptotically stable for any $\tau > 0$ (Theorem 3.1.2(1)), implying the time delay τ does not affect its stability.

If (H_{61}) and (H_{62}) are satisfied, then a stability switch occurs (Theorem 3.1.2(6)). When $\tau = 0$, E_2 is either stable, unstable, or it may undergoe a Hopf bifurcation.

Case 3: (There exists two positive equilibrium points E_1,E_2).

We have the same results as in Case 2.

In summary, the time delay τ does not affect the stability of the positive equilibrium points except in Case 1 when assumption (H_{51}) is satisfied. Then the characteristic equation (3.5) has a zero root and a single pair of purely imaginary eigenvalues. In Cases 2 and 3 when (H_{61}) and (H_{62}) are satisfied, then the characteristic equation (3.5) has two pairs of purely imaginary eigenvalues.

Chapter 4

BIFURCATION ANALYSIS

A Bifurcation is a qualitative change in a dynamical system as its parameters pass through a bifurcation (critical) value. The number of parameters which must be varied for the bifurcation to occur is called the codimension of the bifurcation. For example, saddle-node and Hopf bifurcations are codimension one bifurcations, while a Hopf-Zero bifurcation is a codimension two. Center manifold theorem and the normal form approach are two of the fundamental techniques in bifurcation analysis. They are used to reduce the dimension of the system without lossing significant dynamical properties. Then the existence and nature of bifurcations and the stability of the bifurcating solutions are completely determined by analysing the dynamics on the center manifold. In this chapter we use the projection method, the normal form and the center manifold theorems to study the bifurcations of systems (2.2) and (3.1).

4.1 Bifurcations when $\tau = 0$

We found in chapter 2 that under certain conditions, the characteristic equation of system (2.2) has either one zero or one pair of pure imaginary eigenvalues, implying the existence of a steady-state bifurcation or the possibility of the existence of a Hopf bifurcation under respective conditions.

Suppose the existence of a bifurcation at the equilibrium point $(\tilde{N}, \tilde{A})$. The following transformation of variables $N = x_1 + \tilde{N}$ and $A = x_2 + \tilde{A}$ transforms the equilibrium point $(\tilde{N}, \tilde{A})$ to the trivial equilibrium point $(0, 0)$. Expanding $F(N)$ and $G(A)$ up to second order, and substituting into system (2.2) we have

$$\begin{aligned} x_1' &= -(s + rK^1)x_1 + (-\frac{m}{g} - rK^2 + b)x_2 - rh(x_1, x_2) + O(x_1^4 + x_2^4), \\ x_2' &= grK^1x_1 + grK^2x_2 + grh(x_1, x_2) + O(x_1^4 + x_2^4). \end{aligned} \tag{4.1}$$

where

$$h(x_1, x_2) = a_{11}x_1x_2 + a_{20}x_1^2 + a_{02}x_2^2 + a_{12}x_1x_2^2 + a_{21}x_1^2x_2 + a_{03}x_2^3.$$

with

$$\begin{aligned} a_{11} &= F'(\tilde{N})G(\tilde{A}) + F'(\tilde{N})G'(\tilde{A})\tilde{A}, \\ a_{20} &= \frac{1}{2}F''(\tilde{N})G(\tilde{A})\tilde{A}, \\ a_{02} &= F(\tilde{N})G'(\tilde{A}) + \frac{1}{2}F(\tilde{N})G''(\tilde{A})\tilde{A}, \\ a_{12} &= F'(\tilde{N})G(\tilde{A}) + \frac{1}{2}F'(\tilde{N})G''(\tilde{A})\tilde{A}, \\ a_{21} &= \frac{1}{2}F''(\tilde{N})G(\tilde{A}) + \frac{1}{2}F''(\tilde{N})G'(\tilde{A})\tilde{A}, \\ a_{03} &= \frac{1}{2}F(\tilde{N})G''(\tilde{A}). \end{aligned}$$

Rewrite (4.1) as

$$x' = Ax + F(x), \tag{4.2}$$

where

$$A = \begin{pmatrix} -s - rK^1 & -\dfrac{m}{g} - rK^2 + b \\ grK^1 & grK^2 \end{pmatrix}, \quad x = \begin{pmatrix} x_1 \\ x_2 \end{pmatrix}, \quad F(x) = \begin{pmatrix} -rh(x_1, x_2) \\ grh(x_1, x_2) \end{pmatrix}.$$

The characteristic equation of the linearized system $x' = Ax$ is

$$\lambda^2 + (s + rK^1 - grK^2)\lambda + rK^1 m - sgrK^2 - grK^1 b = 0 \tag{4.3}$$

To do the bifurcation analysis, we choose s as the perturbation parameter for system (2.2) and fix the other parameter values.

4.1.1 Saddle-Node Bifurcation

Suppose at the parameter value $s = s_0$ the following two conditions

$$\frac{K^2}{K^1} = \frac{m - bg}{gs_0} \quad \text{and} \quad K^2 < \frac{s_0 + rK^1}{gr}$$

are satisfied. Then system (2.2) has a nonhyperbolic equilibrium point $(\tilde{N}, \tilde{A})$, with one zero $(\lambda_1 = 0)$ and one negative $(\lambda_2 = -s_0 - rK^1 + grK^2)$ eigenvalue (From (4.3)).

We use the projection method to compute the one-dimensional center manifold.

From$(\lambda_1 I - A)q = 0$, the eigenvector corresponding to$\lambda_1 = 0$ is $q = \begin{pmatrix} 1 \\ \dfrac{gs_0}{bg - m} \end{pmatrix}$.

Let $p = (p_1, p_2)^T \in R^2$ be the adjoint eigenvector. Then

$$p = \begin{pmatrix} \dfrac{grK^2}{grK^2 - s_0 - rK^1} \\ \dfrac{K^2(s_0 + rK^1)}{K^1(grK^2 - s_0 - rK^1)} \end{pmatrix} \text{ satisfying } < p, q >= 1.$$

where $< ., . >$ is the standard scalar (inner) product in R^2.

We have the following Lemma From [33].

Lemma 4.1.1. *Fredholm Alternative: Let T^{su} denote an 1-dimensional linear eigenspace of A corresponding to the negative eigenvalue $\lambda_2 < 0$. Then $y \in T^{su}$ if and only if $< p, y >= 0$.*

Let $y = (y_1, y_2)^T \in R^2$ such that $< p, y >= 0$. Using Lemma 4.1.1, we can decompose any vector $x \in R^2$ as $x = uq + y$ with $uq \in T^c$, $y \in T^{su}$, where T^c is the complementary space of T^{su} in R^2. If q and p are normalized as above, one can get the explicit expressions for u and y. Since $u =< p, x >$, $y = x - < p, x > q$ we have

$$u' =< p, x' >=< p, F(uq + y) >$$

Since $F(uq + y) = O(u^2)$, using Taylor expression, we have

$$u' = \frac{1}{2}\sigma u^2 + O(u^3) = f(u).$$

When the lowest order term is nonzero, we can choose $y = 0$. Then

$$\begin{aligned} \sigma &= \frac{\partial^2}{\partial u^2} < p, F(uq + y) > \Big|_{u=0, y=0} \\ &= 2(a_{02}\frac{g^2 s_0^2}{(bg - m)^2} - a_{11}\frac{gs_0}{bg - m} + a_{20})\frac{grs_0K^2}{K^1(grK^2 - s_0 - rK^1)}. \end{aligned} \tag{4.4}$$

If $\sigma \neq 0$, then $f'(u) = 0, f''(u) \neq 0$, hence, Theorem 3.1 in [33] implies the existence of invertible coordinate and parameter changes transforming system (4.2) into

$$\eta' = \beta \pm \eta^2 + O(\eta^3),$$

where $\beta \in R$ is a perturbation parameter. This system is locally topologically equivalent near the origin to one of the normal forms $\eta' = \beta \pm \eta^2$ (Theorem 3.2 in [33]), implying the existence of a saddle-node bifurcation near the origin.

4.1.2 Hopf Bifurcation

Suppose at the parameter value $s = s_1$ the following two conditions

$$K^2 = \frac{s_1 + rK^1}{gr} \quad \text{and} \quad \frac{K^2}{K^1} > \frac{m - bg}{gs_1}$$

are satisfied, then the Jacobian matrix A in (4.2) has one pair of purely imaginary eigenvalues $\lambda_{1,2} = \pm i\omega_0, \omega_0 = \sqrt{s_1 grK^2 + rK^1(bg - m)}$.

Differentiating the characteristic equation (4.3) with respect to s gives

$$(2\lambda + s + rK^1 - grK^2)\frac{d\lambda(s)}{ds} = grK^2 - \lambda,$$

Hence,

$$\frac{d\lambda}{ds} = \frac{grK^2 - \lambda}{2\lambda + s + rK^1 - grK^2},$$

$$\left.\frac{d\lambda}{ds}\right|_{s=s_1, \lambda=\pm i\omega_0} = -\frac{1}{2} \mp \frac{grK^2}{2\omega_0} i,$$

which implies the existence of Hopf bifurcation at $s = s_1$ since

$$Re\frac{d\lambda}{ds}\bigg|_{s=s_1,\lambda=\pm i\omega_0} = \alpha'(s_1) = -\frac{1}{2} < 0.$$

Similar to the procedure in Section 4.1 , we transfer system (2.2) to system (4.2) where

$$A = \begin{pmatrix} -s_1 - rK^1 & -\frac{m}{g} - rK^2 + b \\ grK^1 & grK^2 \end{pmatrix}, \quad F(x) = \begin{pmatrix} -rh(x_1, x_2) \\ grh(x_1, x_2) \end{pmatrix}.$$

Let $q = (q_1, q_2)^T$ be the eigenvector corresponding to $\lambda_1 = i\omega_0$. Then,

$$q = \begin{pmatrix} -\frac{s_1 + rK^1}{grK^2} + \frac{\omega_0}{grK^1}i \\ 1 \end{pmatrix} = \begin{pmatrix} c \\ 1 \end{pmatrix},$$

where

$$c = -\frac{s_1 + rK^1}{grK^2} + \frac{\omega_0}{grK^1}i = -\frac{grK^2}{grK^1} + \frac{\omega_0}{grK^1}i = -\frac{K^2}{K^1} + \frac{\omega_0}{grK^1}i.$$

Consider the matrix

$$P = (q, \bar{q}) = \begin{pmatrix} c & \bar{c} \\ 1 & 1 \end{pmatrix},$$

Using the transformation of variable $x = Pz$, system (4.2) becomes

$$\dot{z} = P^{-1}APz + P^{-1}F(Pz) = Bz + G(z),$$

where

$$B = \begin{pmatrix} i\omega_0 & 0 \\ 0 & -i\omega_0 \end{pmatrix},$$

$$G(z) = P^{-1}F(Pz) = \begin{pmatrix} \frac{1}{c-\bar{c}} & -\frac{\bar{c}}{c-\bar{c}} \\ -\frac{1}{c-\bar{c}} & \frac{c}{c-\bar{c}} \end{pmatrix} \cdot \begin{pmatrix} -rh(cz+\bar{c}\bar{z}, z+\bar{z}) \\ grh(cz+\bar{c}\bar{z}, z+\bar{z}) \end{pmatrix} = \begin{pmatrix} \mathbf{g}(z,\bar{z}) \\ \bar{\mathbf{g}}(z,\bar{z}) \end{pmatrix},$$

and

$$\mathbf{g}(z,\bar{z}) = -(\frac{1+g\bar{c}}{c-\bar{c}})rh(cz+\bar{c}\bar{z}, z+\bar{z}).$$

Using Taylor expansion we have

$$\mathbf{g}(z,\bar{z}) = \mathbf{g}_{20}\frac{z^2}{2} + \mathbf{g}_{11}z\bar{z} + g_{02}\frac{\bar{z}^2}{2} + \mathbf{g}_{21}\frac{z^2\bar{z}}{2} + \mathbf{g}_{12}\frac{z\bar{z}^2}{2} + \mathbf{g}_{30}\frac{z^3}{6} + \mathbf{g}_{03}\frac{\bar{z}^3}{6} + \text{h.o.t.}$$

where

$$\begin{aligned}
\mathbf{g}_{20} &= -2r(\frac{1+g\bar{c}}{c-\bar{c}})(a_{20}c^2 + a_{11}c + a_{02}), \\
\mathbf{g}_{11} &= -r(\frac{1+g\bar{c}}{c-\bar{c}})(2a_{20}c\bar{c} + a_{11}(c+\bar{c}) + 2a_{02})), \\
\mathbf{g}_{02} &= -2r(\frac{1+g\bar{c}}{c-\bar{c}})(a_{20}\bar{c}^2 + a_{11}\bar{c} + a_{02}), \\
\mathbf{g}_{21} &= -2r(\frac{1+g\bar{c}}{c-\bar{c}})(a_{12}(\bar{c}+2c) + a_{21}(2c\bar{c}+c^2) + 3a_{03}), \\
\mathbf{g}_{12} &= -2r(\frac{1+g\bar{c}}{c-\bar{c}})(a_{12}(2\bar{c}+c) + a_{21}(\bar{c}^2+2c\bar{c}) + 3a_{03}), \\
\mathbf{g}_{30} &= -6r(\frac{1+g\bar{c}}{c-\bar{c}})(a_{12}c + a_{21}c^2 + a_{03}), \\
\mathbf{g}_{03} &= -6r(\frac{1+g\bar{c}}{c-\bar{c}})(a_{12}\bar{c} + a_{21}\bar{c}^2 + a_{03}).
\end{aligned}$$

Thus we can define the following quantities (from [34])

$$\begin{aligned}
C_1(0) &= \frac{i}{2\omega_0}(\mathbf{g}_{20}\mathbf{g}_{11} - 2|\mathbf{g}_{11}|^2 - \frac{1}{3}|\mathbf{g}_{02}|^2) + \frac{\mathbf{g}_{21}}{2}, \qquad (4.5) \\
\Gamma &= -\frac{Re\{C_1(0)\}}{\alpha'(s_1)}, \\
\Omega &= 2Re\{C_1(0)\}.
\end{aligned}$$

Γ determines the direction of the Hopf bifurcation. The Hopf bifurcation occurs as s crossess s_1 to the right if $\Gamma > 0$ and to the left if $\Gamma < 0$. Ω determines the stability of the bifurcating periodic solutions. The bifurcating periodic solutions are orbitally stable (unstable) if $\Omega < 0 (\Omega > 0)$.

4.2 Bifurcations when $\tau \neq 0$

From the discussion in chapter 3 we found that the time delay τ affects the stability of the positive equilibrium points either when assumptions (H_{61}) and (H_{62}) are satisfied, where Eq.(3.5) has two pairs of pure imaginary eigenvalues at which the transversality condition is satisfied, and a stability switch occurs, or when assumption (H_{51}) is satisfied, where Eq.(3.5) has one zero and one pair of pure imaginary eigenvalues at which the transversality condition is satisfied, and a Hopf-Zero bifurcation occurs.

In this section we perform bifurcation analysis of system (3.1), where we let the time delay τ be the perturbation parameter.

4.2.1 Hopf Bifurcation

We found in chapter 3 that if assumptions (H_{61}), (H_{62}) are satisfied, then Eq.(3.5) has two pairs of purely imaginary eigenvalues $\lambda = \pm i\omega_{\pm}$, at the sequences $\tau_{n,1}$, $\tau_{n,2}$ of the time delay τ, where the transversality condition is satisfied, implying the existence of Hopf-bifurcations when $\tau = \tau_{n,1}$ or $\tau = \tau_{n,2}$.

In this section, we use the same procedure in [35], which is based on the normal form method and the center manifold theory to study the direction and stability of the bifurcating periodic solution.

For convenience, let $\tau = \tilde{\tau} + \mu$, ($\tilde{\tau}$ can be $\tau_{n,1}$ or $\tau_{n,2}$), $\mu \in R$. Then $\mu = 0$ is the Hopf bifurcation value for system (3.1). Choose the phase space as $C = C([-\tilde{\tau}, 0], R^2)$. For $\phi \in C$, let

$$L_\mu \phi = A_1 \phi(0) + B_1 \phi(-\tilde{\tau}), \tag{4.6}$$

where

$$A_1 = \begin{pmatrix} -s - rK^1 & -\dfrac{m}{g} - rK^2 \\ grK^1 & grK^2 \end{pmatrix}, \quad B_1 = \begin{pmatrix} 0 & b \\ 0 & 0 \end{pmatrix},$$

By the Riesz representation theorem, there exists a matrix whose components are bounded variation functions $\eta(\theta, \mu)$ in $\theta \in [-\tilde{\tau}, 0]$ such that

$$L_\mu \phi = \int_{-\tilde{\tau}}^{0} d\eta(\theta, \mu)\phi(\theta), \quad \text{for } \phi \in C. \tag{4.7}$$

In fact, we can choose

$$\eta(\theta, \mu) = \begin{cases} A_1 & \theta = 0, \\ -B_1 \delta(\theta + \tilde{\tau}) & \theta \in [-\tilde{\tau}, 0). \end{cases}$$

where δ is defined by $\delta(\theta) = \begin{cases} 0 & \theta \neq 0, \\ 1 & \theta = 0. \end{cases}$, Then (4.7) is satisfied.

For $\phi \in C^1$, define

$$A(\mu)\phi = \begin{cases} \dfrac{d\phi(\theta)}{d\theta} & \theta \in [-\tilde{\tau}, 0], \\ \int_{-\tilde{\tau}}^{0} d\eta(t, \mu)\phi(t) & \theta = 0. \end{cases}$$

and

$$R\phi = \begin{cases} 0 & \theta \in [-\tilde{\tau}, 0], \\ F(\phi) & \theta = 0. \end{cases}$$

Hence, we can rewrite system (3.1) as the following form

$$x_t' = A(\mu)x_t + Rx_t, \tag{4.8}$$

where

$$A(0) = \begin{pmatrix} -s - rK^1 & -\dfrac{m}{g} - rK^2 + be^{i\tilde{\omega}\tilde{\tau}} \\ grK^1 & grK^2 \end{pmatrix}, \text{ and } x_t(\theta) = x(t+\theta), \text{ for } \theta \in [-\tilde{\tau}, 0].$$

For $\psi \in C^1[0, \tilde{\tau}]$, define

$$A^*\phi(s) = \begin{cases} -\dfrac{d\psi(s)}{ds} & s \in [0, \tilde{\tau}], \\ \int_{-\tilde{\tau}}^{0} d\eta(t,0)\psi(-t) & s = 0. \end{cases}$$

Define the bilinear form

$$< \psi, \phi >= \bar{\psi}(0)\phi(0) - \int_{-\tilde{\tau}}^{0}\int_{\xi=0}^{\theta} \bar{\psi}(\xi - \theta)d\eta(\theta)\phi(\xi)d\xi, \tag{4.9}$$

where $\eta(\theta) = \eta(\theta, 0)$. Then A^* and $A(0)$ are adjoint operators.

We have $\lambda_{1,2} = \pm i\tilde{\omega}$ ($\tilde{\omega}$ can be ω_+ or ω_-) are eigenvalues of $A(0)$, thus they are also eigenvalues of A^*. By direct computation, we obtain that

$$q(\theta) = \begin{pmatrix} 1 \\ M \end{pmatrix} e^{i\tilde{\omega}\theta}, \quad \text{where } M = -\frac{g^2r^2K^1K^2}{\tilde{\omega}^2 + g^2r^2K^{2^2}} - i\frac{grK^1\tilde{\omega}}{\tilde{\omega}^2 + g^2r^2K^{2^2}},$$

is the eigenvector of $A(0)$ corresponding to $i\tilde{\omega}$; and

$$q^*(s) = D \begin{pmatrix} \bar{M} \\ 1 \end{pmatrix}^T e^{i\tilde{\omega}s},$$

is the eigenvector of A^* corresponding to $-i\tilde{\omega}$. From $< q^*, q >= 1$, we have

$$D = [2\bar{M} - b\tilde{\tau}\bar{M}^2 e^{i\tilde{\omega}\tilde{\tau}}]^{-1}.$$

Define

$$z(t) =< q^*, x_t > \quad , \quad W(t,\theta) = x_t(\theta) - 2Re\{z(t)q(\theta)\}.$$

On the center manifold

$$W(t,\theta) = W(z(t),\bar{z}(t),\theta) = W_{20}(\theta)\frac{z^2}{2} + W_{11}(\theta)z\bar{z} + W_{02}(\theta)\frac{\bar{z}^2}{2} + W_{30}(\theta)\frac{z^3}{6} + ...$$

z and $\bar{z}$ are local coordinates for center manifold in the direction of q^* and $\bar{q}^*$.

Then at $\mu = 0$,

$$\begin{aligned} \dot{z}(t) &= i\tilde{\omega}z + < q^*(\theta), F(0, W(z,\bar{z},0) + 2Re\{z(t)q(\theta)\}) > \\ &= i\tilde{\omega}z + \bar{q}^*(0)F(0, W(z,\bar{z},0) + 2Re\{z(t)q(0)\}) \qquad (4.10) \\ &= i\tilde{\omega}z + \mathbf{g}(z,\bar{z}). \end{aligned}$$

where

$$\begin{aligned} \mathbf{g}(z,\bar{z}) &= \bar{q}^*(0)F(0, W(z,\bar{z},0) + 2Re\{z(t)q(0)\}) \qquad (4.11) \\ &= \mathbf{g}_{20}\frac{z^2}{2} + \mathbf{g}_{11}z\bar{z} + \mathbf{g}_{02}\frac{\bar{z}^2}{2} + \mathbf{g}_{21}\frac{z^2\bar{z}}{2} + ... \end{aligned}$$

By (4.8) and (4.10), we have

$$\begin{aligned} \dot{W} &= \dot{x}_t - \dot{z}q - \dot{\bar{z}}\bar{q} = \begin{cases} AW - 2Re\{\bar{q}^*(0)Fq(\theta)\}, & \theta \in [-\tilde{\tau}, 0), \\ AW - 2Re\{\bar{q}^*(0)Fq(\theta)\} + F, & \theta = 0. \end{cases} \\ &= AW + H(z,\bar{z},\theta) \end{aligned}$$

Expanding

$$H(z,\bar{z},\theta) = H_{20}(\theta)\frac{z^2}{2} + H_{11}(\theta)z\bar{z} + H_{02}(\theta)\frac{\bar{z}^2}{2} + ... \tag{4.12}$$

and comparing the coefficients, we obtain

$$(A-2i\tilde{\omega}I)W_{20}(\theta) = -H_{20}(\theta), AW_{11}(\theta) = -H_{11}(\theta), (A+2i\tilde{\omega}I)W_{02}(\theta) = -H_{02}(\theta) \tag{4.13}$$

Notice that $q^*(0) = D(\bar{M}, 1)$, and

$$x_t(\theta) = x(t+\theta) = W(t,\theta) + zq(\theta) + \bar{z}\bar{q}(\theta) \Rightarrow x(t) = W(t,0) + zq(0) + \bar{z}\bar{q}(0),$$

hence, $x_1(t) = z + \bar{z} + W_{20}^1(0)\frac{z^2}{2} + W_{11}^1(0)z\bar{z} + W_{02}^1(0)\frac{\bar{z}^2}{2} + ...$ and

$$x_2(t) = Mz + \bar{M}\bar{z} + W_{20}^2(0)\frac{z^2}{2} + W_{11}^2(0)z\bar{z} + W_{02}^2(0)\frac{\bar{z}^2}{2} + ...$$

Finally, we have

$$\begin{aligned}
\mathbf{g}(z,\bar{z}) &= \bar{q}^*(0)F \\
&= \bar{D}(M,1)\begin{pmatrix} -rh(x_1(t),x_2(t)) \\ grh(x_1(t),x_2(t)) \end{pmatrix} \\
&= \bar{D}(g-M)rh(x_1(t),x_2(t)) \\
&= r\bar{D}(g-M)[a_{20}x_1^2 + a_{11}x_1x_2 + a_{02}x_2^2 + a_{21}x_1^2x_2 + a_{12}x_1x_2^2 + a_{03}x_2^3] + h.o.t \\
&= r\bar{D}(g-M)\{(2a_{11}M + 2a_{20} + 2a_{02}M^2)\frac{z^2}{2} + (a_{11}[M+\bar{M}] + 2a_{20} + 2a_{02}M\bar{M})z\bar{z} + \\
&\quad (2a_{11}\bar{M} + 2a_{20} + 2a_{02}\bar{M}^2)\frac{\bar{z}^2}{2} + (2a_{12}M^2 + 4a_{12}M\bar{M} + 2a_{21}\bar{M} + 6a_{03}M^2\bar{M} + \\
&\quad [2a_{20} + a_{11}\bar{M}]W_{20}^1(0) + [a_{11} + 2a_{02}\bar{M}]W_{20}^2(0) + [2a_{11}M + 4a_{20}]W_{11}^1(0) + \\
&\quad [2a_{11} + 4a_{02}M]W_{11}^2(0))\frac{z^2\bar{z}}{2}\}.
\end{aligned}$$

Comparing the coefficients with (4.11), we have

$$
\begin{aligned}
\mathbf{g}_{20} &= r\bar{D}(g-M)(2a_{11}M+2a_{20}+2a_{02}M^2),\\
\mathbf{g}_{11} &= r\bar{D}(g-M)(a_{11}[M+\bar{M}]+2a_{20}+2a_{02}M\bar{M}),\\
\mathbf{g}_{02} &= r\bar{D}(g-M)(2a_{11}\bar{M}+2a_{20}+2a_{02}\bar{M}^2),\\
\mathbf{g}_{21} &= r\bar{D}(g-M)(2a_{12}M^2+4a_{12}M\bar{M}+2a_{21}\bar{M}+6a_{03}M^2\bar{M}+[2a_{20}+a_{11}\bar{M}]W_{20}^1(0)+\\
&\quad [a_{11}+2a_{02}\bar{M}]W_{20}^2(0)+[2a_{11}M+4a_{20}]W_{11}^1(0)+[2a_{11}+4a_{02}M]W_{11}^2(0)).
\end{aligned}
$$

We still need to compute $W_{20}(\theta)$ and $W_{11}(\theta)$, for $\theta \in [-\tilde{\tau}, 0)$. From

$$
\begin{aligned}
H(z,\bar{z},\theta) &= -2Re\{\bar{q}^*(0)Fq(\theta)\}\\
&= -\mathbf{g}q(\theta)-\bar{\mathbf{g}}\bar{q}(\theta)\\
&= -\left(\mathbf{g}_{20}\frac{z^2}{2}+\mathbf{g}_{11}z\bar{z}+\mathbf{g}_{02}\frac{\bar{z}^2}{2}+\ldots\right)q(\theta)-\left(\bar{\mathbf{g}}_{20}\frac{\bar{z}^2}{2}+\bar{\mathbf{g}}_{11}z\bar{z}+\bar{\mathbf{g}}_{02}\frac{z^2}{2}+\ldots\right)\bar{q}(\theta)
\end{aligned}
$$

comparing the coefficients with (4.12) gives that

$$H_{20}(\theta) = -\mathbf{g}_{20}q(\theta)-\bar{\mathbf{g}}_{02}\bar{q}(\theta), \text{ and } H_{11}(\theta) = -\mathbf{g}_{11}q(\theta)-\bar{\mathbf{g}}_{11}\bar{q}(\theta).$$

It follows from (4.13) that

$$\dot{W}_{20}(\theta) = 2i\tilde{\omega}W_{20}(\theta)-\mathbf{g}_{20}q(0)e^{i\tilde{\omega}\theta}-\bar{\mathbf{g}}_{02}\bar{q}(0)e^{-i\tilde{\omega}\theta}.$$

Solving for $W_{20}(\theta)$, we obtain

$$W_{20}(\theta) = \frac{\mathbf{g}_{20}}{i\tilde{\omega}}q(0)e^{i\tilde{\omega}\theta}-\frac{\bar{\mathbf{g}}_{20}}{3i\tilde{\omega}}\bar{q}(0)e^{-i\tilde{\omega}\theta}+E_1e^{2i\tilde{\omega}\theta}, \tag{4.14}$$

and similarly

$$W_{11}(\theta) = \frac{\mathbf{g}_{11}}{i\tilde{\omega}}q(0)e^{i\tilde{\omega}\theta}-\frac{\bar{\mathbf{g}}_{11}}{i\tilde{\omega}}\bar{q}(0)e^{-i\tilde{\omega}\theta}+E_2. \tag{4.15}$$

where E_1 and E_2 are both two-dimensional vectors, and can be determined by setting $\theta = 0$ in H. In fact, since

$$H(z,\bar{z},0) = -2Re\{\bar{q}^*(0)Fq(0)\} + F,$$

we have

$$H_{20}(0) = -\mathbf{g}_{20}q(0) - \bar{\mathbf{g}}_{02}\bar{q}(0) + \begin{pmatrix} -r(2a_{11}M + 2a_{20} + 2a_{02}M^2) \\ gr(2a_{11}M + 2a_{20} + 2a_{02}M^2) \end{pmatrix}, \tag{4.16}$$

and

$$H_{11}(0) = -\mathbf{g}_{11}q(0) - \bar{\mathbf{g}}_{11}\bar{q}(0) + \begin{pmatrix} -r(a_{11}(M+\bar{M}) + 2a_{20} + 2a_{02}M\bar{M}) \\ gr(a_{11}(M+\bar{M}) + 2a_{20} + 2a_{02}M\bar{M}) \end{pmatrix}. \tag{4.17}$$

From (4.13) we have

$$A_1W_{20}(0) + B_1W_{20}(-\tilde{\tau}) = 2i\tilde{\omega}W_{20}(0) - H_{20}(0), \tag{4.18}$$

and

$$A_1W_{11}(0) + B_1W_{11}(-\tilde{\tau}) = -H_{11}(0). \tag{4.19}$$

Substituting (4.14) into (4.18) we have

$$\begin{pmatrix} -s - rK^1 - 2i\tilde{\omega} & -\dfrac{m}{g} - rK^2 + be^{-2i\tilde{\omega}\tilde{\tau}} \\ grK^1 & grK^2 - 2i\tilde{\omega} \end{pmatrix} E_1 = -\mathbf{g}_{20}q(0) - \bar{\mathbf{g}}_{20}\bar{q}(0) - H_{20}(0).$$

Substituting (4.16) into this, we get

$$\begin{pmatrix} -s - rK^1 - 2i\tilde{\omega} & -\dfrac{m}{g} - rK^2 + be^{-2i\tilde{\omega}\tilde{\tau}} \\ grK^1 & grK^2 - 2i\tilde{\omega} \end{pmatrix} E_1 = \begin{pmatrix} r(2a_{11}M + 2a_{20} + 2a_{02}M^2) \\ -gr(2a_{11}M + 2a_{20} + 2a_{02}M^2) \end{pmatrix}.$$

Solving this equation for $(E_1^{(1)}, E_1^{(2)})^T = E_1$, we obtain

$$E_1^{(1)} = \frac{r(2a_{11}M + 2a_{20} + 2a_{02}M^2)(bge^{-2i\tilde{\omega}\tilde{\tau}} - 2i\tilde{\omega})}{-sgrK^2 - 4\tilde{\omega}^2 - 2(-s - rK^1 + grK^2)i\tilde{\omega} + rK^1(m - bge^{-2i\tilde{\omega}\tilde{\tau}})},$$

$$E_1^{(2)} = \frac{gr(2a_{11}M + 2a_{20} + 2a_{02}M^2)(s + 2i\tilde{\omega})}{-sgrK^2 - 4\tilde{\omega}^2 - 2(-s - rK^1 + grK^2)i\tilde{\omega} + rK^1(m - bge^{-2i\tilde{\omega}\tilde{\tau}})}.$$

Similarly, we can get

$$\begin{pmatrix} -s - rK^1 & -\frac{m}{g} - rK^2 + b \\ grK^1 & grK^2 \end{pmatrix} E_2 = \begin{pmatrix} r(a_{11}(M + \bar{M}) + 2a_{20} + 2a_{02}M\bar{M}) \\ -gr(a_{11}(M + \bar{M}) + 2a_{20} + 2a_{02}M\bar{M}) \end{pmatrix}$$

and hence,

$$E_2^{(1)} = \frac{r(a_{11}(M + \bar{M}) + 2a_{20} + 2a_{02}M\bar{M})(bg - m)}{rK^1(m - bg) - sgrK^2},$$

$$E_2^{(2)} = \frac{sgr(a_{11}(M + \bar{M}) + 2a_{20} + 2a_{02}M\bar{M})}{rK^1(m - bg) - sgrK^2}.$$

Based on the above analysis, we can see that each g_{ij} in (4.10) is determined by the parameters and the delay $\tilde{\tau}$. Similarly we can obtain the values of $C_1(0)$, Γ, and Ω in (4.5). If $\Gamma > 0$ (< 0), then the Hopf bifurcation is supercritical (subcritical) and the bifurcating periodic solutions exist for $\tau > \tilde{\tau}$ ($< \tilde{\tau}$). Furthermore, the bifurcating periodic solutions are orbitally stable (unstable) if $\Omega < 0, (> 0)$.

4.2.2 Hopf-Zero Bifurcation

We fix all the parameter values of system (3.1) except s and τ, and assume that at the parameter values $s = s_0$ and $\tau = \tau_{n,1}$, (H_{51}) is satisfied,i.e,

$$\frac{K^2}{K^1} = \frac{m - bg}{gs_0} \quad \text{and} \quad \frac{(s_0 + rK^1 - grK^2)^2}{2rgb} < K^1$$

Then Eq.(3.5) has a single zero and a simple pure imaginary eigenvalue.

By time rescaling, $t \longrightarrow \frac{t}{\tau}$, the system

$$x_1'(t) = -(s + rK^1)x_1 - (\frac{m}{g} + rK^2)x_2 + bx_2(t - \tau) - rh(x_1, x_2) + h.o.t$$
$$x_2'(t) = grK^1x_1 + grK^2x_2 + grh(x_1, x_2) + h.o.t$$

becomes

$$\begin{aligned} x_1'(t) &= \tau[-(s + rK^1)x_1 - (\frac{m}{g} + rK^2)x_2 + bx_2(t - 1) - rh(x_1, x_2)] + h.o.t \quad (4.20) \\ x_2'(t) &= \tau[grK^1x_1 + grK^2x_2 + grh(x_1, x_2)] + h.o.t \end{aligned}$$

We can check that the linearized system

$$x_1'(t) = \tau[-(s + rK^1)x_1 - (\frac{m}{g} + rK^2)x_2 + bx_2(t - 1)],$$
$$x_2'(t) = \tau[grK^1x_1 + grK^2x_2],$$

has a simple zero eigenvalue and a simple pair of pure imaginary eigenvalues under assumption (H_{51}) at $\tau = \tilde{\tau} = \frac{\alpha\tilde{\omega}}{\gamma sin\tilde{\omega}}$, where $\tilde{\omega}$ solves $\tilde{h}(\omega) = \gamma\alpha^2 cos\omega - \gamma^2 sin^2\omega + \beta\alpha^2$, and $\alpha = s_0 + rK^1 - grK^2, \beta = rK^1m - s_0grK^2, \gamma = -grbK^1$.

Therefore, the local center manifold near the origin is in a three-dimensional subspace.

Let $\tau = \tilde{\tau} + \mu_1$, $s = s_0 + \mu_2$ then Eq.(4.20) can be rewritten as

$$x_1'(t) = (\tilde{\tau} + \mu_1)[-(s_0 + \mu_2 + rK^1)x_1 - (\frac{m}{g} + rK^2)x_2 + bx_2(t - 1) - rh(x_1, x_2)] + h.o.t$$
$$x_2'(t) = (\tilde{\tau} + \mu_1)[grK^1x_1 + grK^2x_2 + grh(x_1, x_2)] + h.o.t$$

To obtain the center manifold, we use the bilinear form

$$< \psi, \phi >= \bar{\psi}(0)\phi(0) - \int_{-\tau_{n,1}}^{0} \int_0^\theta \bar{\psi}(\xi - \theta)d\eta(\theta)\phi(\xi)d\xi$$

to decompose C as $C = P \bigoplus Q$, where P is an invariant finite dimensional subspace and Q is the associated invariant infinite dimensional complementary subspace, and $\eta(\theta)$ is a bounded invariant function.

We choose the basis in P as $\Phi(\theta) = (\phi_1, \phi_2, \phi_3)$,where

$$\phi_1 = \begin{pmatrix} 1 \\ M \end{pmatrix} e^{i\tilde{\omega}\theta}, \quad \phi_2 = \bar{\phi}_1 \quad , \quad \phi_3 = \begin{pmatrix} 1 \\ \frac{gs_0}{bg-m} \end{pmatrix},$$

with $$M = -\frac{g^2r^2K^1K^2}{\tilde{\omega}^2 + g^2r^2K^{2^2}} - \frac{grK^1}{\tilde{\omega}^2 + g^2r^2K^{2^2}}\tilde{\omega}i,$$

the basis in Q can be obtained as $\Psi(s) = col(\psi_1, \psi_2, \psi_3)$ with $\psi_1 = d_1{\phi_1}^T$, $\psi_2 = \bar{\psi}_1$, $\psi_3 = d_2{\phi_3}^T$.

Then from $< \Psi, \Phi >= I$ we can determine the values of d_1, d_2 as

$$d_1 = (1 + M\bar{M} - \tilde{\tau}_{n,1}\bar{M}be^{-i\tilde{\omega}\tilde{\tau}})^{-1},$$
$$d_2 = (1 + \frac{g^2s_0^2}{(m-bg)^2} + \frac{gs_0}{m-bg}b\tilde{\tau})^{-1}.$$

Hence the dynamical behavior of the system is determined by

$$x' = Bx + \Psi(0)F(\Phi x, \mu) \tag{4.21}$$

where

$$B = \begin{pmatrix} i\tilde{\omega} & 0 & 0 \\ 0 & -i\tilde{\omega} & 0 \\ 0 & 0 & 0 \end{pmatrix}$$

$$
\begin{aligned}
F(\varphi,\mu) &= \mu_1 \begin{pmatrix} -(s_0+rK^1)\varphi_1(0) - (\frac{m}{g}+rK^2)\varphi_2(0) + b\varphi_2(-1) \\ grK^1\varphi_1(0) + grK^2\varphi_2(0) \end{pmatrix} \\
&+ \mu_2 \begin{pmatrix} \tilde{\tau}\varphi_1(0) \\ 0 \end{pmatrix} + \tilde{\tau} \begin{pmatrix} -rh(\varphi_1(0),\varphi_2(0)) \\ grh(\varphi_1(0),\varphi_2(0)) \end{pmatrix} + h.o.t
\end{aligned}
$$

$$
\Psi(0) = \begin{pmatrix} d_1 & d_1M \\ \bar{d}_1 & \bar{d}_1\bar{M} \\ d_2 & \frac{gs_0}{bg-m}d_2 \end{pmatrix}.
$$

We can further reduce Eq.(4.21) to the normal form

$$
\begin{aligned}
x_1' &= i\tilde{\omega}x_1 + m_{11}x_1 + m_{12}x_1x_3 + h.o.t \\
x_2' &= -i\tilde{\omega}x_2 + \bar{m}_{11}x_2 + \bar{m}_{12}x_2x_3 + h.o.t \\
x_3' &= m_{21}x_3 + m_{22}(x_3^2 + 2x_1x_2) + h.o.t
\end{aligned} \tag{4.22}
$$

where

$$
\begin{aligned}
m_{11} &= d_1\mu_1[-(s_0+rK^1) - (\frac{m}{g}+rK^2)M + grM(K^1+MK^2) + bMe^{-i\tilde{\omega}} + \mu_2\tilde{\tau}], \\
m_{12} &= rd_1\tilde{\tau}(gM-1)[2a_{20} + a_{11}M + (a_{11}+2a_{20}M)\frac{gs_0}{bg-m}], \\
m_{21} &= d_2\mu_2\tilde{\tau}, \\
m_{22} &= -rd_2\tilde{\tau}(\frac{g^2s}{m-bg}+1)(a_{20} - a_{11}\frac{gs}{m-bg} + a_{02}\frac{g^2s^2}{(m-bg)^2}).
\end{aligned} \tag{4.23}
$$

Using the transformations

$$
\begin{cases} x_1 = \omega_1 + i\omega_2 \\ x_2 = \omega_1 - i\omega_2 \\ x_3 = \omega_3 \end{cases} \quad \text{and} \quad \begin{cases} \omega_1 = \rho cos\xi \\ \omega_2 = \rho sin\xi \\ x_3 = z \end{cases}
$$

subsequently, we can change Eq.(4.22) to real then cylindrical coordinates,

$$\begin{aligned}
\dot{\rho} &= Re(m_{11})\rho + Re(m_{12})z\rho + h.o.t, \\
\dot{\zeta} &= \tilde{\omega} + h.o.t, \\
\dot{z} &= m_{21}z + m_{22}(z^2 + 2\rho^2) + h.o.t.
\end{aligned} \tag{4.24}$$

Since $Re(m_{12})$, $m_{22} \neq 0$ (note that m_{22} is real), the higher-order terms have no qualitative effects. Therefore, we have the following conclusion.

Theorem 4.2.1. *If the parameters satisfy assumption (H_{51}), and $\tau = \tau_{n,1}$, then the flow of system (3.1) on the local center manifold is given in cylindrical coordinates by (4.24).*

Chapter 5

NUMERICAL SIMULATION

In this chapter we provide numerical simulations to illustrate our theoretical predictions in the previous chapters by choosing functions and parameter values satisfying the hypothesis. For instance, we choose the two particular functions $F(N) = \frac{N}{N+1}$ and $G(A) = \frac{A}{A^2+1}$ which satisfy conditions (C_1) and (C_2). Obviously, the maximum value of $G(A)$ is $\frac{1}{2}$ at $A = A^* = 1$. In real ecological systems the parameter values are usually lying in certain regions provided in the following table (see [36])

Symbol	Description	Reported range
L	The rate of N input	0.00005-0.26$gCm^{-3}day^{-1}$
s	The rate of N output due to respiration and sedimentation	0.0008-0.13 day^{-1}
r	The maximum per capita grazing rate	0.5-1.5$gCm^{-3}day^{-1}$
b	The phytoplankton respiration rate	0.05-0.15 day^{-1}
g	Conversion rate of nutrient into phytoplankton	0.5-1.5$gCm^{-3}day^{-1}$
m	The phytoplankton mortality rate	0.0828-0.36 day^{-1}

In the numerical simulations, we fix $L = 0.200$, $r = 0.700$, $b = 0.100$, $g = 1.000$, $m = 0.250$, then $\frac{m}{gr} = 0.357 < G(A^*)$, and choose s as a perturbation parameter.

In the following we use the dynamical package XPPAUT to examine the bifurcations and to integrate and observe trajectories of systems (2.2) and (3.1).

5.1 Bifurcations when $\tau = 0$

From the discussion in Section 4.1 we know that when s is chosen as a perturbation parameter, then system (2.2) undergoes either a saddle-node or Hopf bifurcations, which are codimension one bifurcations, under certain conditions. The following bifurcation diagrams illustrate how the dynamical behavior of system (2.2) changes as the parameter s is varied

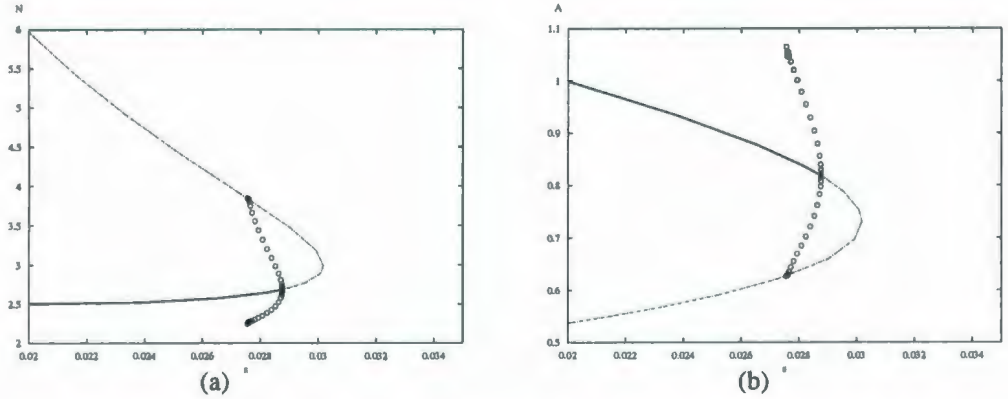

Figure 5.1: The bifurcation diagrams of (a) N vs s, and (b) A vs s.

In Figure (5.1), the solid line denotes stable equilibrium points, and the dashed line denotes unstable ones. The filled circles represent the appearance of stable periodic orbits and open circles represent the appearance of unstable ones. Obviously, as s increases there is change either in the number or stability of the positive equilibrium points.

When s is relatively small ($s \in [0, 0.0276)$), there exist two positive equilibrium points, E_1 is unstable (saddle) point, and E_2 is locally asymptotically stable. For example, at $s = 0.025$, $E_1 = (4.450, 0.600)$ and $E_2 = (2.600, 0.860)$. Figure (5.2) shows the trajectories of system (2.2) for initial conditions near the positive equilibrium points. Obviously, they all approach to the equilibrium point E_2, it indicates that E_1 is unstable and E_2 is locally asymptotically stable

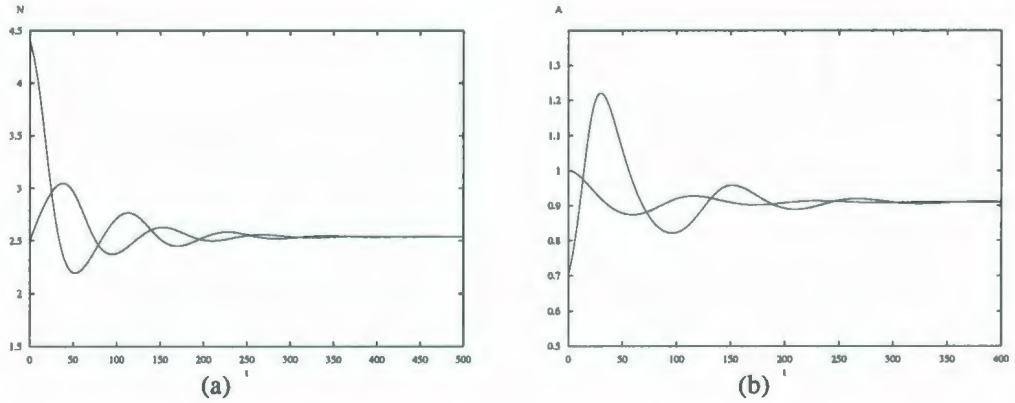

(a) (b)

Figure 5.2: Trajectories of system (2.2) for $s = 0.025$.IC $(N, A) = (4.4, 0.7), (2.5, 1.0)$.

When s increases to the intermediate value ($s \in (0.0276, 0.0284)$) , the system possesses multistability. More specifically, in addition to the existence of stable or unstable solutions, we observe the appearance of unstable periodic orbits. For example, when $s = 0.028$, Figure (5.3) shows that the solution could be stable, unstable, or becomes unstable periodic, depending on the initial condition.

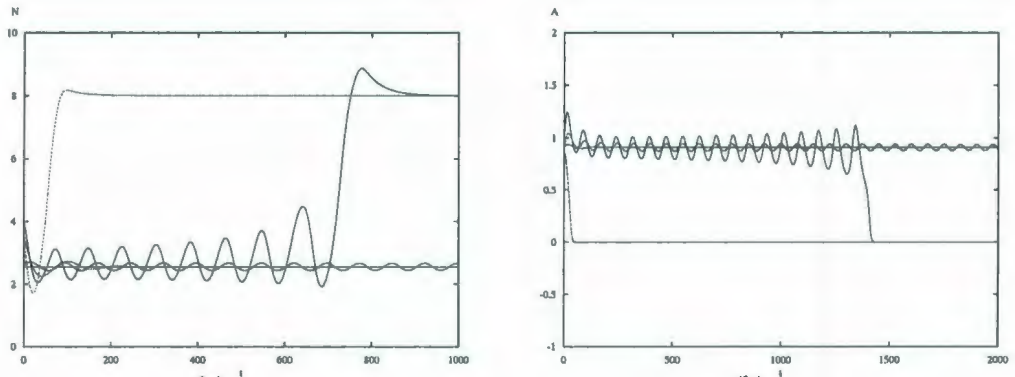

Figure 5.3: Trajectories of system (2.2) for $s = 0.028$. IC$(N, A) = (4.0, 0.7), (2.5, 0.8), (2.6, 0.9)$, Here the horizontal line represents the equilibrium point.

For higher s values ($s \in (0.0284, 0.030)$), E_1 keeps unstable while E_2 becomes unstable. For instance, when $s = 0.029$, we can obtain $E_1 = (3.45, 0.64)$, $E_2 = (2.80, 0.80)$, Figure (5.4) shows that both of them are unstable. All the near-by trajectories approach to the boundary equilibrium point.

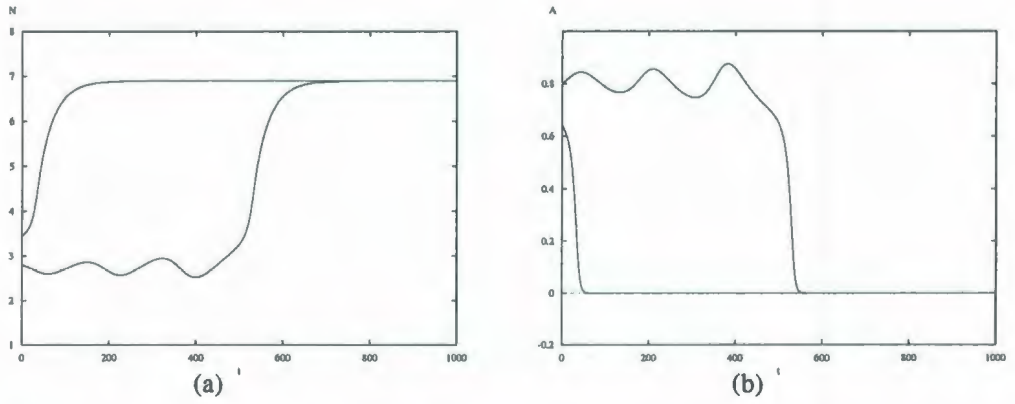

Figure 5.4: Trajectories of system (2.2) for $s = 0.029$.IC(N, A)=$(3.5, 0.65), (2.82, 0.82)$

Finally when s is big enough ($s > 0.030$), the only equilibrium point is the boundary equilibrium point E_0 which is globally asymptotically stable. Figure (5.5) shows the global stability of E_0 at $s = 0.031$

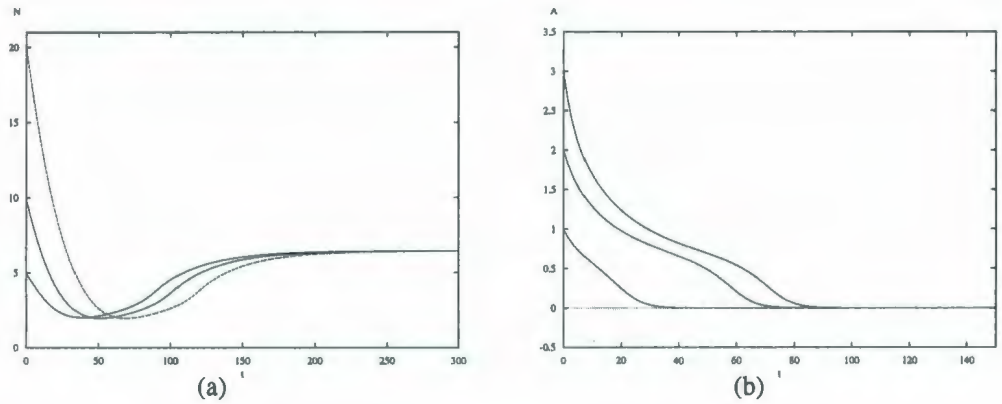

Figure 5.5: Trajectories of system (2.2).IC $(N, A) = (5.0, 1.0), (10, 2.0), (20, 3.0)$.

It is obvious from the previous figures that when the nutrient output rate s is small enough, the system has two positive equilibrium points, one is an unstable (saddle) point, and the other is locally asymptotically stable. For higher s values the system exhibits multistability, where unstable periodic solutions occur. If the parameter s increased further, the stable equilibrium point loses its stability. When s is big enough, then the two positive equilibrium points disappear, and the boundary equilibrium point is the only equilibrium point which is globally asymptotically stable.

Since the number of the positive equilibrium points changes from two to zero as s crosses the critical parameter value $s_0 = 0.030$, and E_2 change its stability from stable to unstable at $s_1 = 0.0284$, bifurcations occur at the critical points $s = s_0$ and $s = s_1$. In the following, we discuss these bifurcations in detail.

Saddle-Node Bifurcation

It is clear from Figure (5.1) that when $s > s_0$, there is no positive equilibrium point, and when $s < s_0$ there exists two positive equilibrium points E_1,E_2, implying the existence of

a saddle-node bifurcation.

The following figure shows the nullclines and the phase portrait of system (2.2) at $s = s_0$

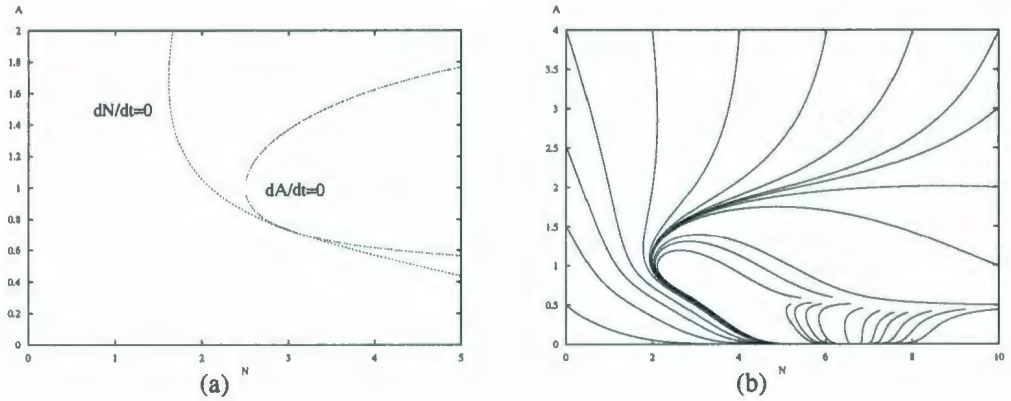

Figure 5.6: (a) The nullclines, and (b) the phase portrait of system (2.2) for $s = 0.030$.

It is obvious from Figure (5.6) that there exists only one positive equilibrium point $E_1 = (N_1^*, A_1^*) = (3.000, 0.730)$, which is unstable. We can calculate $\frac{K_1^2}{K_1^1} = \frac{m - bg}{gs_0} = 5.000$ and $K_1^2 = 0.054 < \frac{s_0 + rK_1^1}{gr} = 0.065$, which confirms the existence of saddle-node bifurcation (see Section 4.1.1). In fact, we have $maxH(A) = 0.357$ at $A = \hat{A} = 0.740$, satisfying $H(\hat{A}) = \frac{m}{gr}$, so it belongs to Case 1 in Table 2.1, also, we can calculate the two eigenvalues $\lambda_1 = 0, \lambda_2 = 0.008$.

Increasing s slightly, for example at $s = 0.035 > s_0$, figure (5.7) shows the nullclines and the phase portrait

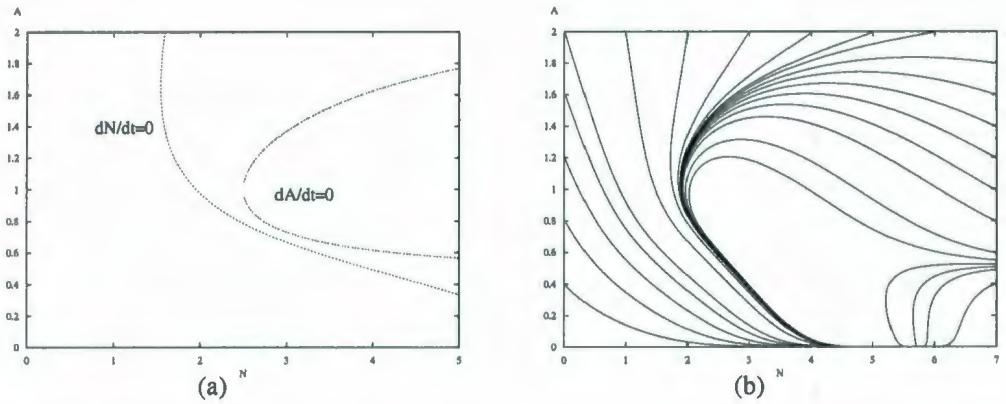

Figure 5.7: (a) The nullclines, and (b) the phase portrait of system (2.2) for $s = 0.035$.

Clearly, the only equilibrium point is the boundary equilibrium point $E_0 = (\frac{L}{s}, 0) = (5.714, 0)$ which is globally asymptotically stable. Furthermore, we can check that $H(\hat{A}) = H(0.700) = 0.340$, then $H(\hat{A}) < \frac{m}{gr}$, so it corresponds to Case 0 in Table 2.1.

If we choose $s = 0.025 < s_0$, then the nullclines and the phase portrait of system (2.2) are depicted in Figure (5.8)

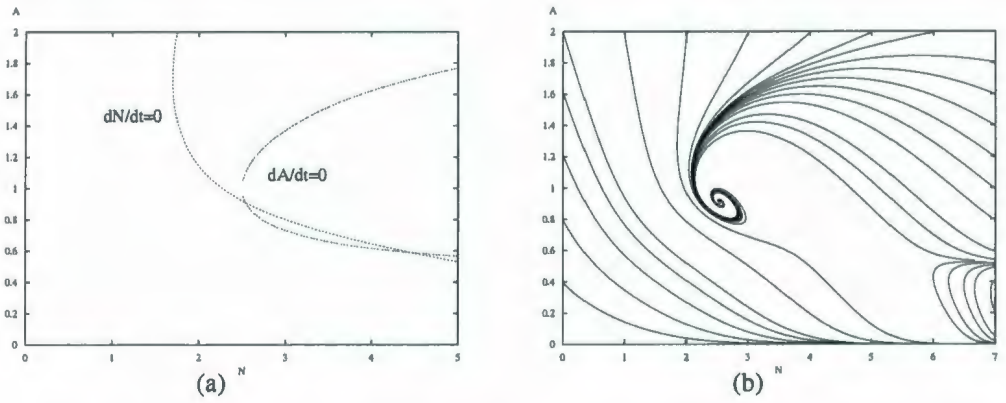

Figure 5.8: (a) The nullclines, and (b) the phase portrait of system (2.2) for $s = 0.025$.

Obviously there exists two positive equilibrium points $E_1 = (4.450, 0.600)$, which is a

saddle point and $E_2 = (2.600, 0.860)$ which is locally asymptotically stable. Similarly, we can calculate $H(\hat{A}) = H(0.700) = 0.375$, $H(A^*) = 0.333$, which satisfies $H(A^*) < \frac{m}{gr} < H(\hat{A})$, therefore, it belongs to Case 2 in Table 2.1.

The previous figures confirm the change of the number of the positive equilibrium points from two to zero as the parameter s crosses the critical parameter value s_0 to the right, indicating the existence of saddle-node bifurcation at $s = s_0$.

Hopf Bifurcation

We notice from Figure (5.1) that the unstable branch emanates from Hopf bifurcation at the critical parameter value $s_1 = 0.0284$ and bends to the left, while the steady state solution loses the stability to the right. Therefore, Hopf bifurcation is subcritical, implying that when s is decreased there exists periodic solution which is unstable (corresponds to the open circles in Figure (5.1)). In fact, we can calculate the first Liapunov coefficient at $s = s_1$, $\Omega = 1.8 > 0$ (from (4.5)) indicate that the bifurcating periodic solutions are unstable.

Actually, we can check that at $s = s_1$, system (2.2) has two positive equilibrium points, $E_1 = (3.650, 0.640)$ which is a saddle point, and $E_2 = (2.650, 0.840)$ which satisfies $K_2^2 = \frac{s_1 + rK_2^1}{gr} = 0.045$ and $\frac{K_2^2}{K_2^1} = 9.000 > \frac{m - bg}{gs_1} = 5.357$, implying the existence of a Hopf Bifurcation (see Section 4.1.2).

When we choose $s = 0.028 < s_1$, then from the discussion in the first part of this section we know that the system exhibits multistability at this parameter value (see Figure (5.3). The phase portrait is depicted in Figure (5.9)

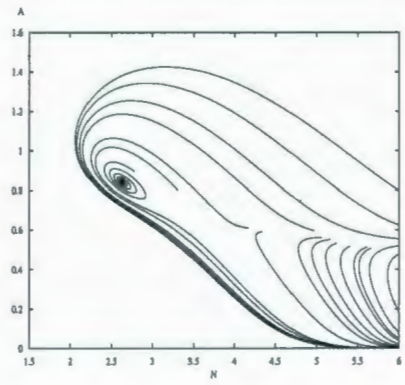

Figure 5.9: The phase portrait of system (2.2) for $s = 0.028$.

From the biological point of view, when the nutrient output rate (s) is very small, there exists a stable steady-state with high phytoplankton density and low nutrient density, implying high probability of the occurance of phytoplankton bloom. As the nutrient output rate increases, the phytoplankton biomass decreases rapidly, whereas the nutrient biomass increases slowly, at this stage, the bloom declines. However, when the nutrient output rate reaches a proper value, the system becomes oscillatory, then the phytoplankton concentration can increase abruptly to reach levels much higher than those attained by any steady-state value, which corresponds to the occurance of the bloom. When the nutrient output rate is big enough, the nutrient concentration becomes very small to a degree that it can't support the phytoplankton growth, hence, the phytoplankton go to extinction. Therefore, the phytoplankton bloom can be controlled by increasing the nutrient outpout rate. This can be achieved by precipitating the nutrient to the sediments using chemical treatment, then by removing these sediments to prevent nutrients from being recycled again into the water system.

5.2 Bifurcations when $\tau \neq 0$

We know from the discussion in Section 4.2 that because of the involvement of the time delay, system (3.1) exhibits rich dynamical properties which may not occur in the system without delay. If we choose the time delay τ as a bifurcation parameter of system (3.1), then much more interesting dynamical behavior can be observed. For example, stability switches occur under assumptions (H_{61}) and (H_{62}). Then at a sequence of critical values of τ, there exist Hopf bifurcations with different amplitudes in the oscillatory trajectories. Similar to the system without time delay, when we take s as the first bifurcation parameter of system (3.1), a steady-state bifurcation occurs, the combination of the steady-state bifurcation and the Hopf bifurcation at a critical value of τ yields a Hopf-Zero bifurcation under assumption (H_{51}), which is a codimension two bifurcation.

Stability Switches

We recall from Section 4.2.1 that if assumptions

$(H_{61}) : K^1m - sgK^2 > max\{gbK^1, \frac{(s+rK^1-grK^2)^2}{2r}\}$, and

$(H_{62}) : (s+rK^1-grK^2)^2((s+rK^1-grK^2)^2-4r(K^1m-sgK^2))+4g^2r^2K^{1^2}b^2 > 0$

are satisfied, then stability switches occur in system (3.1) at two sequences of critical values of $\tau = \tau_{n,1}, \tau_{n,2}$.

First, we choose $s_2 = 0.025$, then system (2.2) has two positive equilibrium points, $E_1 = (4.450, 0.600)$, and $E_2 = (2.600, 0.860)$, when $\tau = 0$, E_1 is a saddle point and E_2 is locally asymptotically stable.

At E_2, we can calculate $K_2^1m-s_2gK_2^2 = 0.007, gbK_2^1 = 0.003, \frac{(s_2+rK_2^1-grK_2^2)^2}{2r} =$

8×10^{-5}, implying $K_2^1 m - s_2 g K_2^2 > max\{gbK_2^1, \frac{(s_2 + rK_2^1 - grK_2^2)^2}{2r}\}$, and $(s_2+rK_2^1-grK_2^2)^2((s_2+rK_2^1-grK_2^2)^2-4r(K_2^1m-s_2gK_2^2))+4g^2r^2K_2^{1^2}b^2=97\times10^{-4}> 0$. Therefore, assumptions (H_{61}) and (H_{62}) are satisfied, implying the existence of two purely imaginary roots $\lambda = i\omega_{\pm}$, with $\omega_+ = 0.083$, $\omega_- = 0.051$, at $\tau_{n,1} = \frac{4.124 + 2\pi n}{0.083}$, and $\tau_{n,2} = \frac{4.851 + 2\pi n}{0.051}$, $n = 0, 1, 2, ...$ We can calculate the first couple of the critical values as $\tau_{0,1} = 49.688$, $\tau_{1,1} = 125.389$, $\tau_{2,1} = 201.090$, $\tau_{0,2} = 95.125$, $\tau_{1,2} = 218.325$.

Since $0 < \tau_{0,1} < \tau_{0,2} < \tau_{1,1} < \tau_{2,1} < \tau_{1,2} < ...$ then from Theorem 3.1.2(6) we have that, E_2 is locally asymptotically stable when $\tau \in [0, \tau_{0,1}) \cup (\tau_{0,2}, \tau_{1,1})$ and unstable when $\tau \in (\tau_{0,1}, \tau_{0,2}) \cup (\tau_{1,1}, \infty)$, and there exist Hopf bifurcations at the critical values $\tau_{0,1}, \tau_{0,2}$, and $\tau_{1,1}$. This means that as the delay τ varies, E_2 switches two times from stable to unstable, then to stable, and finally becomes unstable.

Now let τ be a perturbation parameter. When $\tau = 49 \in [0, \tau_{0,1})$. Figure (5.10) shows that E_2 is asymptotically stable, although it converges very slow.

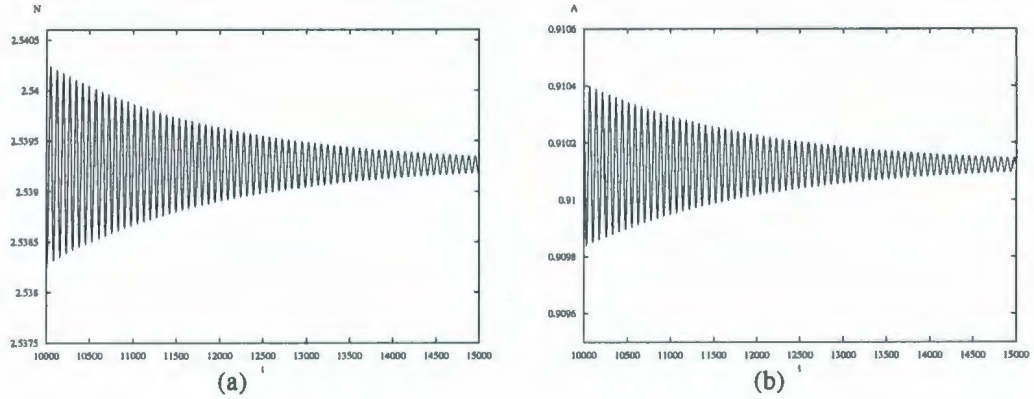

Figure 5.10: The solutions, (a) N vs t, (b) A vs t, when $\tau = 49$.

When $\tau = \tau_{0,1} = 49.688$, there exists a Hopf Bifurcation. Figure (5.11) represents the corresponding periodic solutions.

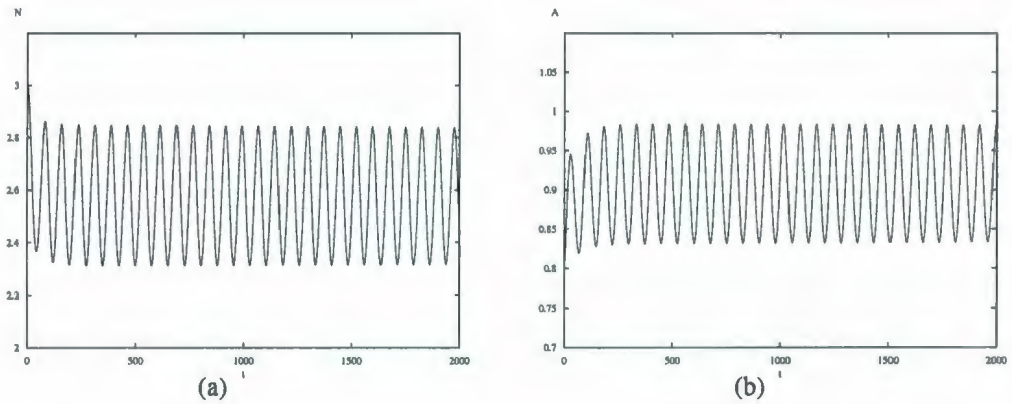

Figure 5.11: The periodic solutions, (a) N vs t, (b) A vs t, when $\tau = \tau_{0,1}$.

The first Liapunov coefficient at $\tau = \tau_{0,1}$ is $\Omega = -1.8 < 0$ implies the appearance of a stable limit cycle.

If $\tau = 50 \in (\tau_{0,1}, \tau_{0,2})$, the solution curves depicted in Figure (5.12) show that E_2 becomes unstable.

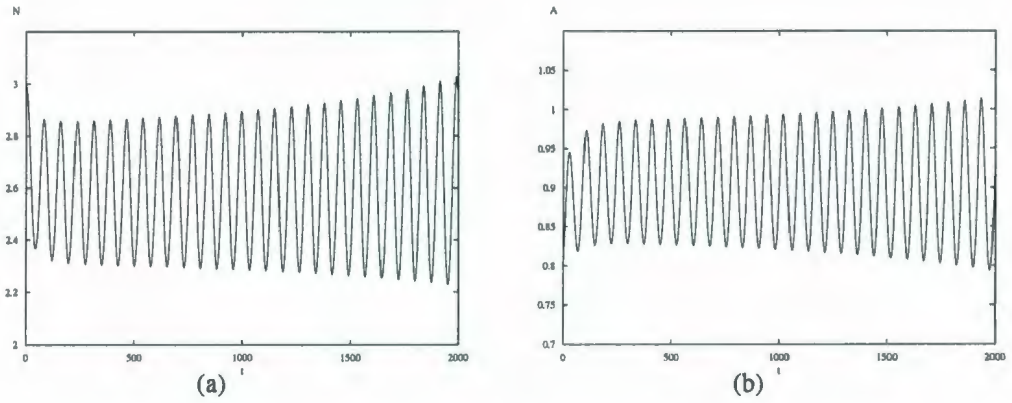

Figure 5.12: The solutions, (a) N vs t, (b) A vs t, when $\tau = 50$.

The first Liapunov coefficient at $\tau = \tau_{0,2}$ is $\Omega = 0.7 > 0$ which confirms the appearance of an unstable limit cycle.

When $\tau = 95.5 \in (\tau_{0,2}, \tau_{1,1})$, E_2 becomes asymptotically stable again. See Figure (5.13)

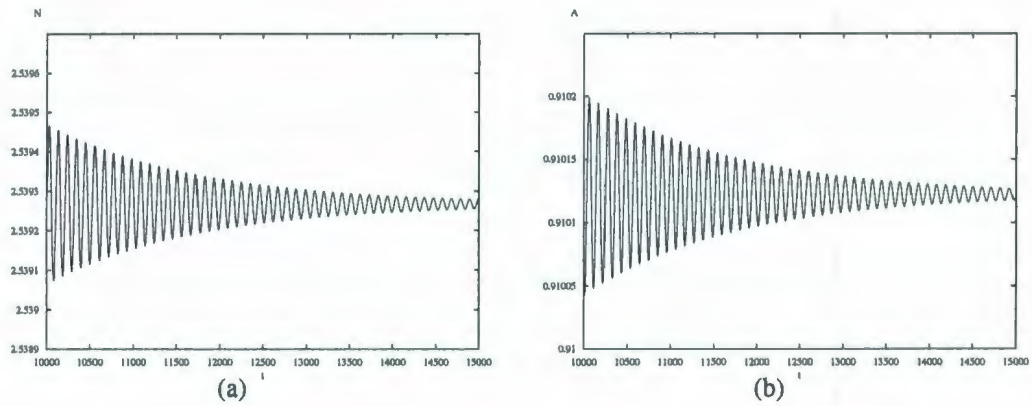

Figure 5.13: The solutions, (a) N vs t, (b) A vs t, when $\tau = 95.5$.

Finally when $\tau > \tau_{1,1}$ the solution loses the stability and remains unstable. Figure (5.14) shows the solution is unstable when $\tau = 140 > \tau_{1,1}$

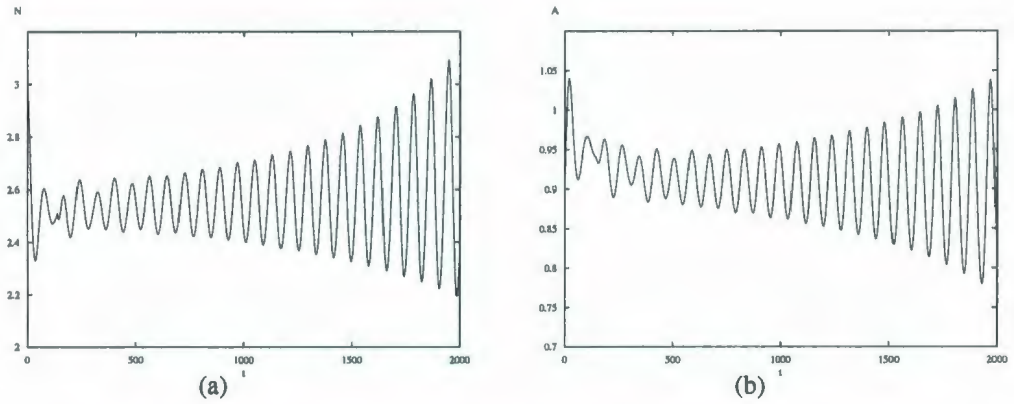

Figure 5.14: The solutions, (a) N vs t, (b) A vs t, when $\tau = 140$.

The previous figures show that when the time delay increases, E_2 switches twice, from stable to unstable, then to stable again, and finally becomes unstable.

Biologically, if the recycling time required to regenerate nutrient from dead phytoplankton biomass is very small, then the stable steady-state keeps its stability, implying that both nutrient and phytoplankton coexist. If the recycling time increases till it crosses the first

critical value, then the steady-state loses its stability, and the amplitudes of the phytoplankton and nutrient becomes oscillatory, with high levels of phytoplankton and low levels of nutrients. However, if the recycling time gets larger, and it crosses the second critical value, the steady state gains its stability again, hence, both of the biomasses can exist equilibriumlly. If the dead phytoplankton biomass is very hard to convert into nutrient, the steady-state becomes unstable again and the phytoplankton disappears. This partially explains the collapse of the bloom during the cold seasons, since the water temperature reaches very low levels, and consequently the time required to regenerate nutrient from dead phytoplankton biomass increases.

Hopf-Zero Bifurcation

We know from Section 4.2.2 that if assumption

$$(H_{51}): \frac{K^2}{K^1} = \frac{m - bg}{gs_0} \quad \text{and} \quad \frac{(s_0 + rK^1 - grK^2)^2}{2rgb} < K^1$$

is satisfied, then system (3.1) undergoes Hopf-Zero bifurcation when $s = s_0$, at a sequence of critical values of $\tau = \tau_{n,1}$.

Let $s_0 = 0.030$, then system (2.2) has one positive equilibrium point $E_1 = (3.000, 0.730)$, which is unstable at $\tau = 0$. We can check $\frac{K_1^2}{K_1^1} = \frac{m - bg}{gs_0} = 5.000$, $\frac{(s_0 + rK_1^1 - grK_1^2)^2}{2rgb} = 6.820 \times 10^{-3} < K_1^1 = 0.022$, hence, condition (H_{51}) is satisfied, implying the existence of a Hopf-Zero bifurcation at the parameter value $\tau_{0,1} = 18.375$.

Since Hopf-Zero bifurcation is a codimension two bifurcation, we choose both s and τ as the bifurcation parameters, and investigate the solutions of system (3.1) near the critical values of $s = s_0$ and $\tau = \tau_{0,1}$.

If we fix $s = s_0$, and choose $\tau = 18.370 < \tau_{0,1}$, E_1 is unstable. See Figure (5.15)

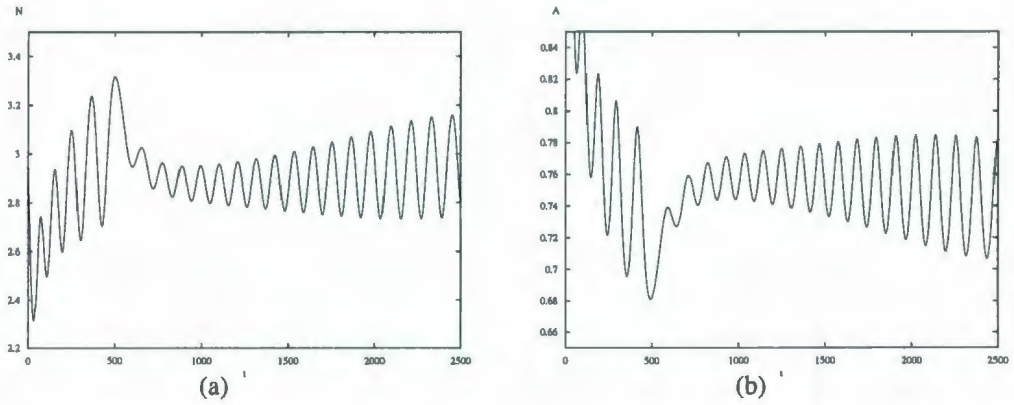

Figure 5.15: The solutions, (a) N vs t, (b) A vs t, when $(s, \tau) = (0.030, 18.370)$.

While for $\tau = 18.380 > \tau_{0,1}$, Figure (5.16) shows that E_1 becomes asymptotically stable.

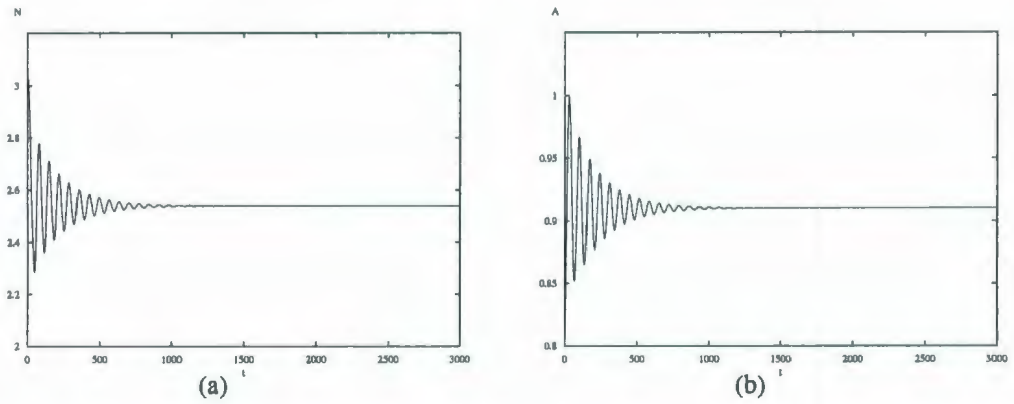

Figure 5.16: The solutions, (a) N vs t, (b) A vs t, when $(s, \tau) = (0.030, 18.380)$.

Chapter 6

CONCLUSION

In this project, we consider a ODE model and a modified DDE model. At first, we present a mathematical model including two ordinary differential equations to describe the nutrient-phytoplankton interactions, where an uptake function which is a generalization of those used by many authors, and instantaneous nutrient recycling are used. The boundedness of the model's solutions is proved, then its dynamical properties are investigated. Our results show the existence of a boundary equilibrium point, and we use geometrical methods to find conditions for the existence of none, one, or at most two positive equilibrium points. After obtaining the equilibrium points, analytical and geometrical methods are used to analyze the local stability of each equilibrium point. We can prove that the boundary equilibrium point is always locally asymptotically stable, and it can be globally asymptotically stable under certain sufficient condition. A conjecture is given for the global stability of the boundary equilibrium point when it is the only equilibrium point (partially proved). If the system has only one positive equilibrium point, then it is degenerate (either stable or unsta-

ble), whereas, when two positive equilibrium points exist, one of them is always a saddle point, while the other one could be either locally asymptotically stable or unstable. The possibility of the existence of saddle-node or Hopf bifurcations under different conditions is discussed.

Second, we modify the previous model by introducing the delayed nutrient recycling. The effect of the time delay on the stability of the equilibrium points is discussed, by investigating the distribution of the roots of the corresponding transcendental characteristic equation. Our result shows that the time delay does not affect the stability of the equilibrium points except when a Hopf-Zero bifurcation or stability switch may occur under certain conditions.

As we vary the parameters, stability may be lost. The system can undergo bifurcations. Therefore, the bifurcations of both the instantaneous system and the system with delay are studied. Particularly, the nutrient output rate is chosen as the bifurcation parameter and the other parameter values are fixed. By using the projection method, the existence of a saddle-node bifurcation for the system without time delay is proved. Furthermore, the normal form approach and the center manifold theorem are used to determine the direction of Hopf bifurcation and the stability of the bifurcating periodic solutions in both systems, and to prove the existence of Hopf-Zero bifurcation for the system with delay.

Numerical simulation results are given to further verify the theoretical predictions. Where the nutrient output rate is used again as a varying parameter. The bifurcation diagrams of the system without delay is given to show the significant change either in the number or stability of the positive equilibrium points as the parameter (nutrient output rate) is varied. The existence of two critical parameter values at which a saddle-node and

Hopf bifurcations occur can be observed from the bifurcation diagrams as well. Moreover, the trajectories with different initial conditions are given to confirm the stability of each positive equilibrium point for different values of the parameter. Furthermore, numerical simulations are given to show the existence of stability switches and the occurance of Hopf-Zero bifurcation for the model with delay.

Biological interpretations based on the bifurcation diagrams of the system are given to gain the insight that the phytoplankton bloom occurs for small nutrient output rate and collapses for high one. Therefore, the phytoplankton bloom can be controlled by keeping the nutrient outpout rate at high level, which can be achieved by using chemicals to precipitate the nutrient to the sediments, then by removing these sediments to prevent nutrients from being recycled again into the water system. Moreover, the time required to regenerate nutrient from dead phytoplankton biomass determines whether both nutrient and phytoplankton coexist, or if they oscillate with high levels of phytoplankton and low levels of nutrients.

Although our model includes the main factors that affect the nutrient-phytoplankton interactions, it can be improved by many ways. For example, we can consider the effect of other biological factors such as higher predation, and physical factors such as light intensity and water temperature. Furthermore, we can add a term which represents the internal nutrient storage to incorporate the fact that phytoplankton consume nutrient in excess of their immediate need, and they continue to grow and divide for quite some time even when the external nutrient is depleted [37, 38]. Moreover, our model can be improved by using periodic nutrient input or distributed delay nutrient recycling.

Bibliography

[1] S.H.Strogatz,*Nonlinear Dynamics and Chaos With Applications to Physics, Biology, Chemistry, and Engineering*,Studies in nonlinearity 1994,Addison-Wesley Publishing Company.

[2] F.Brauer and C.C.Chavez,*Mathematical Models in Population Biology and Epidemiology*, Texts in Applied Mathematics 40 (2001),Springer-Verlag.

[3] H.I.Freedman,*Deterministic Mathematical Models in Population Ecology*, Monographs And Textbooks in Pure and Applied Mathematics, 1980, Marcel Dekker Inc.

[4] H.R.Thieme,*Mathematics in Population Biology*,Princeton Series in Theoretical And Computational Biology, 2003, Princeton University Press.

[5] G.Riley, H.Stammel and D.Burrpus,*Qualitative ecology of the plankton of the Western North Atlantic*, Bull.Bingh.Ocean.Coll,12(1949),1-169.

[6] E.Litchman and C.A.Klausmeier,*Competition of phytoplankton under fluctuating light*, American Naturalist ,157(2001),170-187.

[7] U.Franke, K.Hutter and K.Johnk,*A physical biological coupled model for algal dynamics in lakes*, Bulletin of Mathematical Biology,61(1999),239-272.

[8] M.J.Fasham,P.M.Holligan, and P.R.Pugh,*The spatial and temporal development of the spring phytoplankton bloom in the Celtic Sea*,Prog.Oceanogr,12(1983),87-145.

[9] G.T.Evans,*A framework for discussing seasonal succession and coexistence of phytoplankton species*, Limnology and Oceanography,(1988)33,1027-1036.

[10] B.W.Frost,*Grazing control of phytoplankton stock in the open sub-arctic Pacific Ocean. A model assessing the role of mesozooplankton, particularly the large calanoid copepods neocalanus* Mar.Ecol.Ser, 39(1987),49-68.

[11] G.T.Evans and J.S.Parslow,*A model of annual plankton cycles*,Biol.Oceanogr,3(1985),327-427.

[12] B.C.Patten,*Mathematical models of plankton production*,Hydrobiology,53(1968),357-408.

[13] S.B.Hsu, S.Hubbel and P.Waltman,*A mathematical theory for single-nutrient competition in continuous cultures of micro-organisms*,SIAM J.App.Math,32(1977),366-383.

[14] P.Waltman,S.P.Hubbel and S.B.Hsu,*Theoretical and experimental investigations of microbial competition in continuous culture*,Modeling and differential equations in biology, New York, Dekker,1980.

[15] J.W.Caperon and J. Meyer,*Nitrogen-limited growth of marine phytoplankton I. Changes in population characteristics with steady-state growth rate*Deep-Sea Res,19 (1972),601-618.

[16] T.Powell,P.J.Richerson*Temporal variation, spatial heterogeneity and completion for resources in plankton system: a theoretical model*,American Naturalist,125(1985), 431-464.

[17] G.J.Butler,H.I.Freedman and P.Waltman,*Uniformly persistent systems*,Proc.Am.Math .Soc,96(1986),425-430.

[18] G.J.Butler and G.Wolkowicz,*Global dynamics of a mathematical model of competition in the chemostat:general response functions and different death rates*,SIAM. J.Appl.Math,52(1992),222-233.

[19] R.M.Nisbet and W.S.C.Gurney,*Model of material cycling in a closed ecosystem* Nature, 264(1976),633-635.

[20] R.M.Nisbet,J.McKinstry and W.S.C.Gurney,*A strategic model of material cycling in a closed ecosystem*Math.Biosci,64(1983),99-113.

[21] R.E.Ulanowicz*Mass and energy flow in closed ecosystems*J.Theor.Biol,34(1972),239-253.

[22] T.Powell and P.J.Richerson,*Temporal variation,spatial heterogeneity and competition for resource in plankton system:a theoretical model*American Naturalist,125(1985), 431-464.

[23] S.Ruan,*The effect of delays on stability and persistence in plankton models*,Nonlinear Analysis,Theory,Methods and Applications,Vol.24,No.4,(1995),575-585.

[24] A.Huppert,B.Blasius and L.Stone,*A Model of Phytoplankton Blooms*,The American Naturalist, Vol.159,No.5,February(2002).

[25] Y.Kuang,*Delay Differential Equations with Applications in Population Dynamics*, Academic Press,New York,1993.

[26] C.S.Holling,*Some characteristics of simple types of predation and parasitism.* Canadian Entomologist,91(1959),385-398.

[27] J.Vandermeer and D.E.Goldberg,*Population Ecology, First Principles*, 2003, Princeton University Press.

[28] M.E.Solomon,*The natural control of animal populations*,Journal of Animal Ecology 18,(1949),1-35.

[29] P.C.Fraser and W.Gary,*Type-3 functional response in limnetic suspension-feeders, as demonstrated by in situ grazing rates*,Hydrobiologia,232(1992),175-191.

[30] A.L.Real,*The Kinetics of Functional Response*,The American Naturalist, Vol,111, No,978(1977)289-300.

[31] V.Lenteren and J.C.Bakker,*Functional responses in invertebrates*,Netherlands Journal of Zoology,26 (1976),567-572.

[32] R.H.Whittaker,*Communities and Ecosystems*Macmillan,New York,1975.

[33] Y.A.Kuznetsov,*Elements of Applied Bifurcation Theory*,Applied Mathematical Sciences 112 (1991),Springer-Verlag.

[34] Y.J.Wei and Y.Yuan,*Stability Switches and Hopf Bifurcations in a Pair of Delay-Coupled Oscillators*, J.Nonlinear Science,Vol.17(2)(2007),145-166.

[35] J.Wei and S.Ruan,*Stability and bifurcation in a neural network model with two delays*, Physica D 130(1999),255-272.

[36] A.Edwards and J.Brindley,*Zooplankton Mortality and the Dynamical Behavior of Plankton Population Models*,Bulletin of Mathematical Biology, 61(1999),303-339.

[37] S.Jang and J.Baglama,*Droop models of nutrient-plankton interaction with intratrophic predation*,Applied Mathematics and Computation, 169(2005),1106-1128.

[38] N.Norhayati,A.Ross,G.C.Wake,*A bifurcation analysis of a simple phytoplankton and zooplankton model*,Mathematical and Computer Modelling, 45(2007),449-458.

[39] Y.Yuan and J.Wei,*Singularity Analysis on a Planar System with Multiple Delays*, J.Dynamics and Differential Equations. Vol.19(2)(2007),437-456.

[40] J.J.Wei and Y.Yuan,{Synchronized Hopf Bifurcation Analysis in a Neural Network Model with Delays, J.Mathematical Analysis and Applications Vol.312(2005),205-229.

[41] S.Ruan,*Oscillations in Plankton Models with Nutrient Recycling*,J.theor.Biol,208 (2001),15-26.

[42] M.E.Andrew and J.B.Brindley,*Oscillatory behavior in a three-component plankton population model*, Dynamics and Stability of Systems, Vol.11(4)(1996),347-370.

[43] D.C.Sigee,*Freshwater Microbiology*,John Wiley and Sons,LTD,NJ,USA,2005.

[44] E.Beretta, G.I.Bischi and F.Solimano,*Stability in chemostat equations with delayed nutrient recycling*J.Math.Biol.28(1990),99-111.

[45] S.Ruan and X.Z.He,*Global stability in chemostat type plankton models with delayed nutrient recycling*J.Math.Biol,37(1998),253-271.

[46] J.Hale and H.Kocak,*Dynamics and Bifurcations*, Texts in Applied Mathematics, 3,(1991) Springer-Verlag.

[47] J.Guckenheimer and P.Holmes,*Nonlinear Oscillations, Dynamical Systems, and Bifurcations of Vector Fields*,Applied Mathematical Sciences 42,1983,Springer-Verlag.

[48] K.Gopalsamy,*Stability and Oscillations in Delay Differential Equations of Population Dynamics*, Mathematics and Its Applications,1992, Kluwer Academic Publishers.

[49] M.Kot,*Elements of Mathematical Ecology*, 2001, Cambridge University Press.

[50] D.Neal,*Introduction to Population Biology*, 2004, Cambridge University Press.